QEDC

Quantum Engineering Design Short Term Program

Under the Japan-East Asia Network of Exchange

for Students & Youths (JENESYS) Program

Final Report

Quantum Engineering Design Course
Osaka University, Japan
September, 2011

PREFACE:

For the Fiscal Year 2010, nine (9) young and motivated short-term students from Vietnam, Malaysia, Philippines, Indonesia, Thailand, India, came to Osaka University to experience various research, academic and cultural activities designed under the Quantum Engineering Design Course (QED-C) Short-Term Program, whose aim is to foster research in fields that address environmental issues and technological advancement and to promote cooperation and linkages between Asian countries.

As one of the best features of this program, each student is able to closely interact with Japanese researchers by an assignment to a laboratory under a supervision of professor who is a member of the Quantum Engineering Design Research Initiative Group (QEDRI). The QEDRI group has a large network among academia, industries and agencies, therefore, the students have wider exposure to research frontiers through participation in international conferences, workshops and other scientific forum aside from their direct interaction with other members of their laboratories. Moreover, the cultural and social interaction aspects of the program are integrated through many formal and informal discourse and cultural exchange activities.

This Final Report, therefore, contains both the (1) research/academic achievements and (2) cherished life experiences in Japan of all the students who participated in this 5month or one-year program. It is hoped that these works and experiences of students will serve as guide to young researchers interested in an intensive, research-focused but culturally diverse short-term programs.

Finally, we extend gratitude to Japan-East Asia Network for Students and Youths (JENESYS) program, Japan Student Services Organization (JASSO) and Osaka University for support, the member professors of QEDRI for cooperation, the secretarial and staffs for the students' affairs/support services and most of all to the young students who are unwavering in their participation and "rich" in curiosity to learn and share new things and ideas.

Truly, I thank you all.

Prof. Hideaki Kasai
Osaka, Sept 2011

Quantum Engineering Design Short Term Program 2010
Student List

Student's name/Affiliation/Nationality/ Supervisor in Osaka University

5-month-course: August 2010-December 2010

AL REY VILLAGRACIA - De La Salle University / Philippines
Supervisor: Prof. Hideaki Kasai

CHAIYAPAT TANGPATJAROEN – Chulalongkorn University / Thailand
Supervisor: Prof. Kazuto Yamauchi

INDRA YUDHISTIRA – National University of Singapore / Indonesia
Supervisor: Prof. Yoji Shibutani

12-month-course: October 2010-September 2011

BUI VAN PHO – College of Science, Vietnam National University / Vietnam
Supervisor: Prof. Kazuto Yamauchi

CICA GUSTIANI - Bandung Institute of Technology / Indonesia
Supervisor: Prof. Hideaki Kasai

ELISHA GABRIELLE VERZOSA TIU – De La Salle University / Philippines
Supervisor: Prof. Takashi Kubo

GAGUS KETUT SUNNARDIANTO – University of Indonesia / Indonesia
Supervisor: Prof. Hisazumi Akai

JAGADEESH SURIYA PRAKASH – Anna University / India
Supervisor: Prof. Koun Shirai

MUHAMMAD ASLAM BIN ROSLE – International Islamic University of Malaysia / Malaysia
Supervisor: Prof. Hideaki Kasai

Secretariat

Ikuko Nojiri / Kasai Laboratory / Graduate School of Engineering / Osaka University

Schedule of Quantum Engineering Design Short Term Program 2010

2010.8	Start of 5-month-course
2010.10	Start of 12-month- course Opening Ceremony for the Graduate School of Engineering Orientation of the program by the Advisor for International Students QEDC Welcome Party
2010.12	End of 5-month-course Year-end Party
2011.1	Quantum Engineering Design Course Workshop
2011.2	International Academic Workshop
2011.3	18th Computational Materials Design Workshop at International Institute for Advanced Studies
2010.4	Welcome Party & Cherry-blossom viewing International Workshop on Applied Surface Science/Nanostructures and Fuel Cell Engineering
2011.8	farewell party
2011.9	End of 12-month- course Submission of Final Report of Quantum Engineering Design Short Term Program 2010

2010.10 Opening Ceremony

Opening Ceremony

Orientation of the program

QEDC Welcome Party

2011.1 QED Course Workshop

2011.3 18th CMD Workshop

Preliminary Investigation on Hydrogen and Oxygen Adsorption on Iron Surface (001)

Al Rey C. Villagracia

Abstract

Reactions of iron and magnetite to water are cheap ways for hydrogen gas production that is needed for an alternative source of energy [11-12]. The cyclic transformation of iron to magnetite and magnetite to iron leads to the cyclic production of H_2 and water [2,5,10]. In this study, investigation on hydrogen atom, oxygen atom and hydroxide on the surface on iron (001) are to be used for the dissociation of water on iron. Results showed that hydrogen and oxygen atom would tend to be in the hollow site of iron surface (001) while the hydroxide tends to be in the bridge site of the surface. This information tells us that dissociation of water to OH and H occurs near the bridge site. Due to the limited number of pages, only this portion of study was submitted. OH adsorption, PES of OH and H_2O dissociation on Fe (001), bulk magnetite and magnetite surface (001) were not included [7,9].

I. Introduction

One of the most given attention in present research is the generation of alternative ways of producing energy. Hydrogen Fuel Cell is one of the technologies that can be used for the production of energy. Researchers are developing a wide range of technologies to produce hydrogen economically from a variety of resources in environmentally friendly ways [1-2].

Among these resources, iron was chosen because of its abundance and most specially when oxidized in water naturally forms hydrogen gas and rust is formed on the surface of iron. Above 373 K, rusts are transformed to magnetite and hydrogen gas. At 473 K, iron reacted to water directly forms magnetite on the surface without intermediate formation of rusts [2,5,10]. Moreover, magnetite is induced directly back to iron when reacted with any excess hydrogen gas below 523 K. Equation (1) and Equation (2) summarizes the reaction.

$$Fe_3O_4 + 4H_2 \rightarrow 3Fe + 4H_2O \quad (1)$$

$$3Fe + 4H_2O \rightarrow Fe_3O_4 + 4H_2 \quad (300\,^{\circ}C) \quad (2)$$

There are two types of formation of rusts on the surface of iron in which it depends on the abundance of oxygen. Aerobic corrosion will lead to the formation of $Fe(OH)_2$ (green rusts) and then to $Fe(OH)_3$ (yellow rusts). Anaerobic corrosion will only lead to green rusts. These green rusts when heated above 373 K will transform into magnetite. Yellow rusts when reacted with siderite leads to formation of magnetite [1].

Based on the reactions above, it can be seen that water dissociates to OH and H that will transform to rusts and hydrogen gas. We investigated the adsorption of O and H on the surface of Iron (001). The objective of this study is to determine the adsorption sites of the molecule on the surface of Iron.

II. Computational Method

Spin Polarized Density functional theory (DFT) method was implemented in the calculations with the use of Vienna Ab Initio Simulation Package (VASP) with the use of pseudo potentials.

Iron surface (001) was chosen as the surface for the adsorption of oxygen, hydrogen and hydroxide because of its known stability. To determine the number of layers needed, surface and bulk density of states were compared. In all periodic computations, 5x5x1 k-points and 400 eV energy cut off were used. Isolated systems of oxygen, hydrogen and hydroxide were also simulated. The lattice constant of the crystal body-centered cubic iron bulk was also verified for convergence.

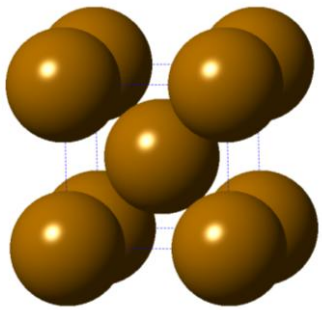

Figure 1 Body-Centered Cubic Iron Bulk

For the adsorption of hydrogen on the iron surface (001), 5 layers and 7 layers of ion (001) were used to check that layers needed for the simulation. Moreover, 1x1 and 2x2 surface sizes were also used to verify the size needed for the simulation. The number of layers and surface size resulted in the hydrogen adsorption were used for the oxygen and hydroxide adsorptions. The super unit cell used in this varies from 2.86x2.86x25 and 5.72x5.72x25.

There are nine sites determined for the adsorption of hydrogen, oxygen and hydroxide on the surface of iron (001). Below is the diagram of the sites on the surface of iron.

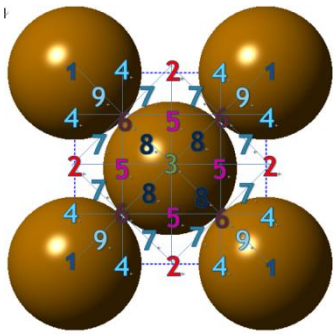

Figure 2 Adsorption sites on Fe(001)

Sites 1, 2 and 3 are commonly known as the top, bridge and hollow site of adsorption. Figure 3 shows the diagram for the adsorption of hydrogen and oxygen on Fe (001).

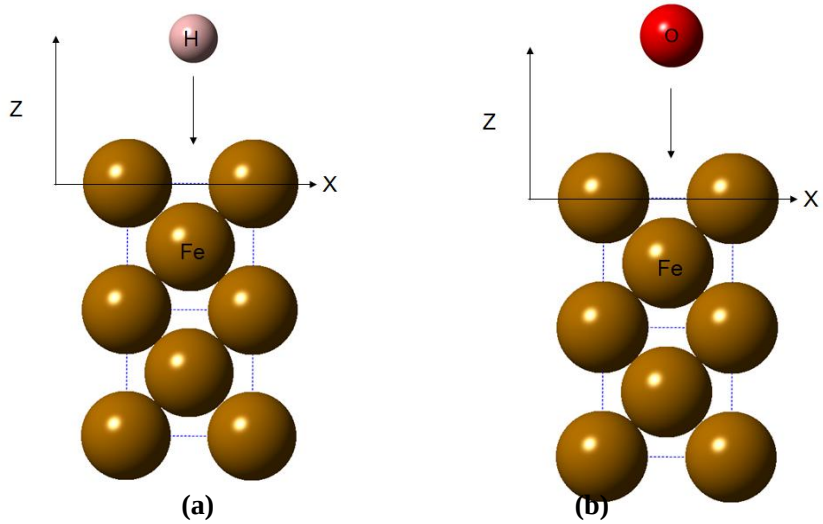

(a) **(b)**

Figure 3 Diagram of Adsorptions on 5L 1x1 Fe (001)

(a) Hydrogen (b) Oxygen

III. Results and Discussion

1) Bulk Iron Calculation

Figures 4, 5 and 6 show the lattice constant convergence test, local density of states and band structure of iron bulk, respectively. Results of the calculation showed an approximate lattice constant of 2.86 Å to experimental value of 2.866 Å.

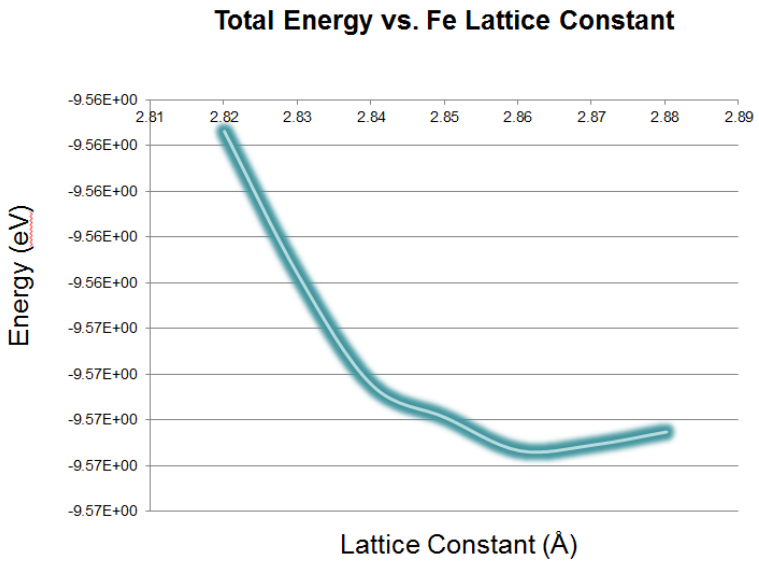

Figure 4 Lattice Constant Convergence Test for Iron

The calculated magnetic moment 2.218 μB is approximately equal to the experimental value of 2.2 μB.

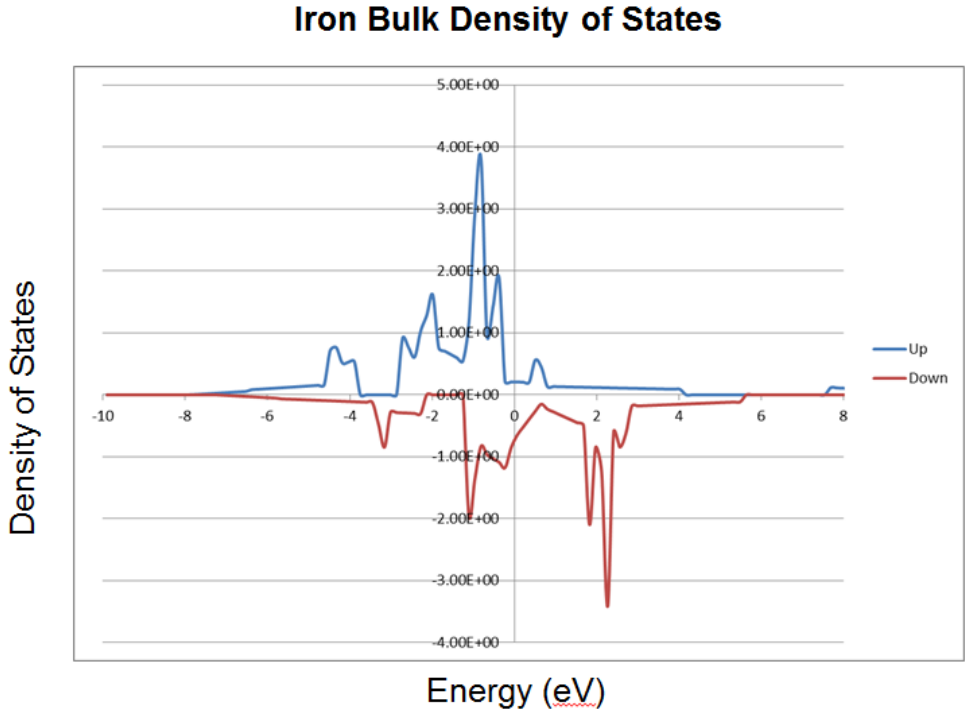

Figure 5 Density of States of Iron

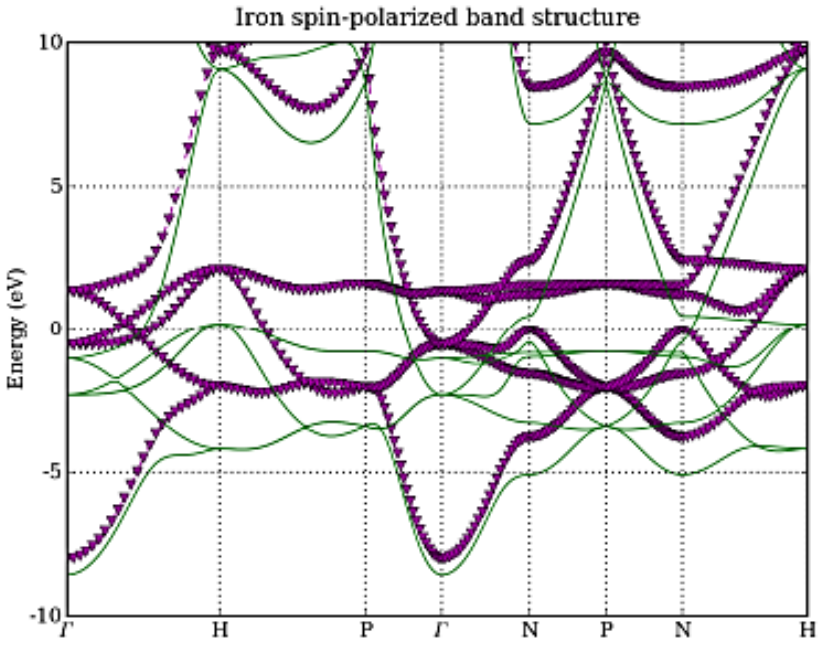

Figure 6 Band Structure of Iron

Figure 4 and 5 validated the conductivity of the iron due to the occupied states across the Fermi level at 0 eV.

2) Surface Layer Calculation

To determine the number of layers needed in the calculation, the density of states of 3 to 7 layers of iron (001) were compared to the bulk density of states. Figure 5 shows the density of states of 5 layers of iron (001) which is sufficient enough to be used for the adsorption calculations. The magnetic moment 2.308 also matched with that of bulk atom. However, hydrogen adsorption on 7 layers was also calculated to confirm this conclusion.

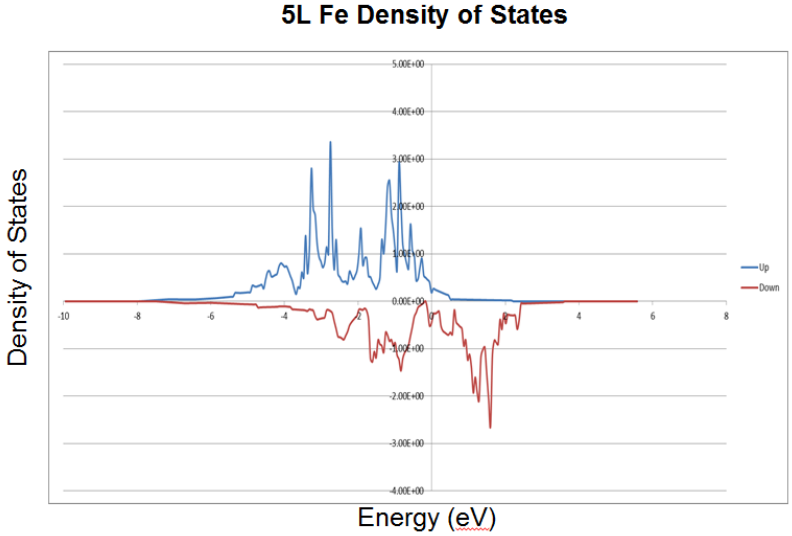

Figure 7 Density of States of Five Layers of Iron (001)

3) Hydrogen Adsorption on Fe (001)

(a) 5 Layers of 1x1 Fe (001)

The binding site shown on Figure 8 can be found in the hollow site at a distance of 0.4 Å with energy of 3.19635 eV. Figure 9 shows that the charges moved from iron surface to hydrogen as expected since the electronegativity of hydrogen is higher than iron. Yellow color on the charge difference shows a positive difference (increase) while cyan color means negative difference (decrease) of charges.

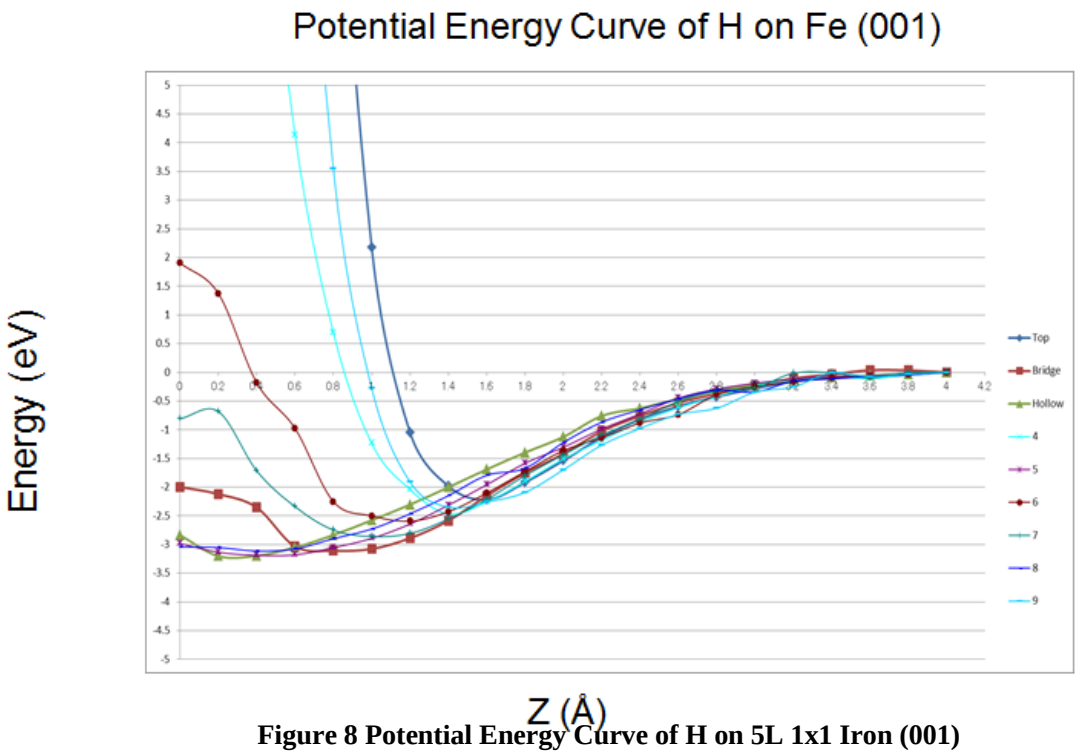

Figure 8 Potential Energy Curve of H on 5L 1x1 Iron (001)

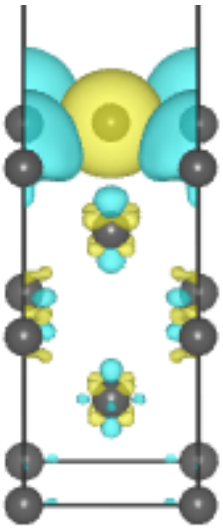

Figure 9 Charge Difference of H on 5L 1x1 Iron (001)

(b) 7 layers of 1x1 Fe (001)

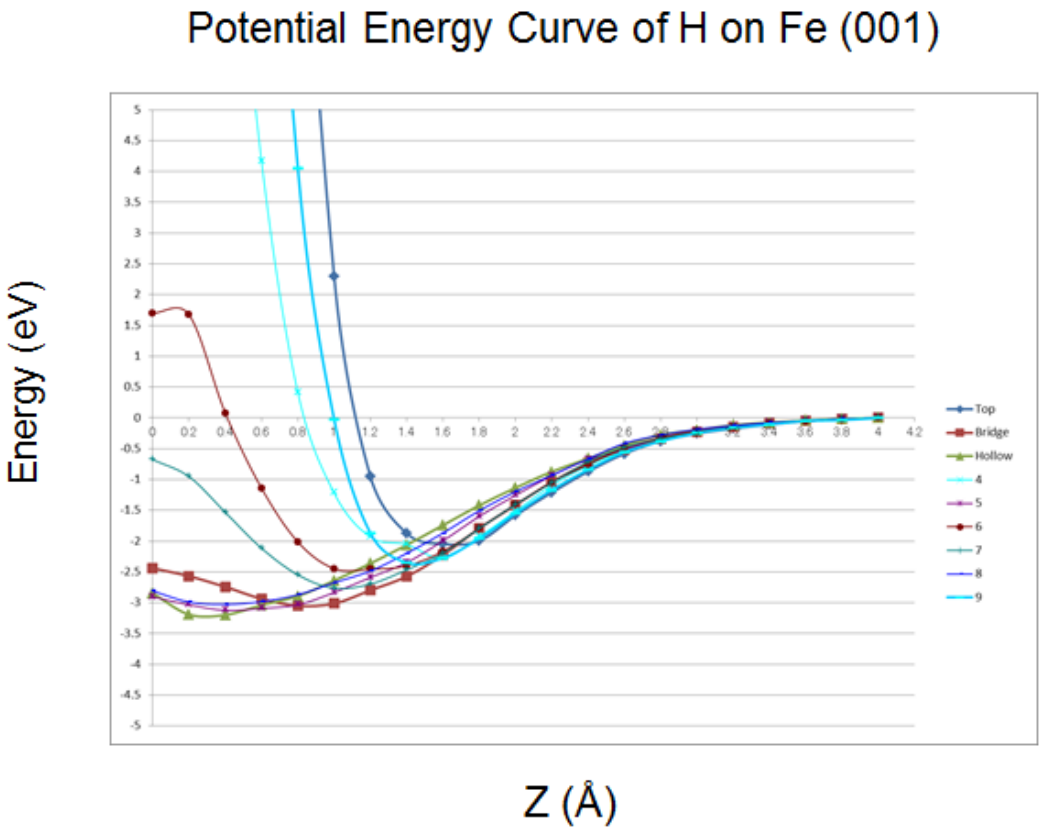

Figure 10 Potential Energy Curve of H on 7L 1x1 Iron (001)

Results in 7 layers of Fe (001) matched with the results in 5 layers of Fe (001). The binding site is found in the hollow site at a distance of 0.40 Å with energy of 3.19774 eV. It means that 5 layers of Fe (001) is enough for the adsorption of hydrogen.

(c) 5 layers of 2x2 Fe (001)

The binding site found in the hydrogen adsorption on 5 layers of 2x2 iron (001) can be found in the hollow site at 0.40 Å with energy of 3.200295 eV as shown in Figure 11. This means that 1x1 iron (001) surface suffices the study of hydrogen adsorption on iron (001). The value obtained matched with other DFT studies [3,7].

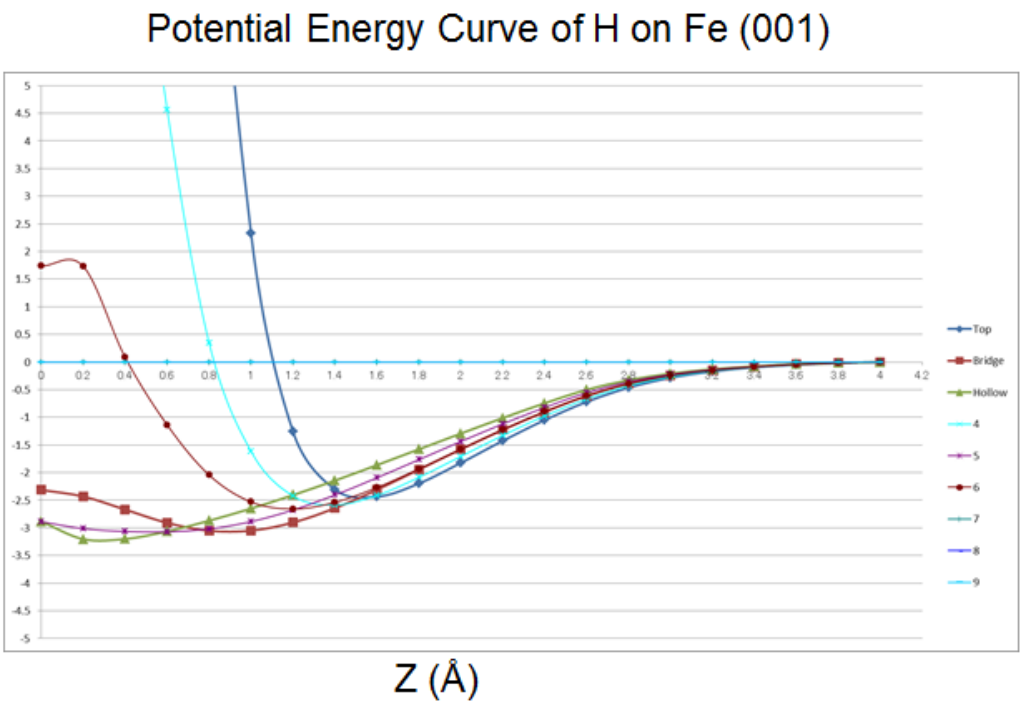

Figure 11 Potential Energy Curve of H on 5L 2x2 Iron (001)

4) Oxygen Adsorption on Fe (001)

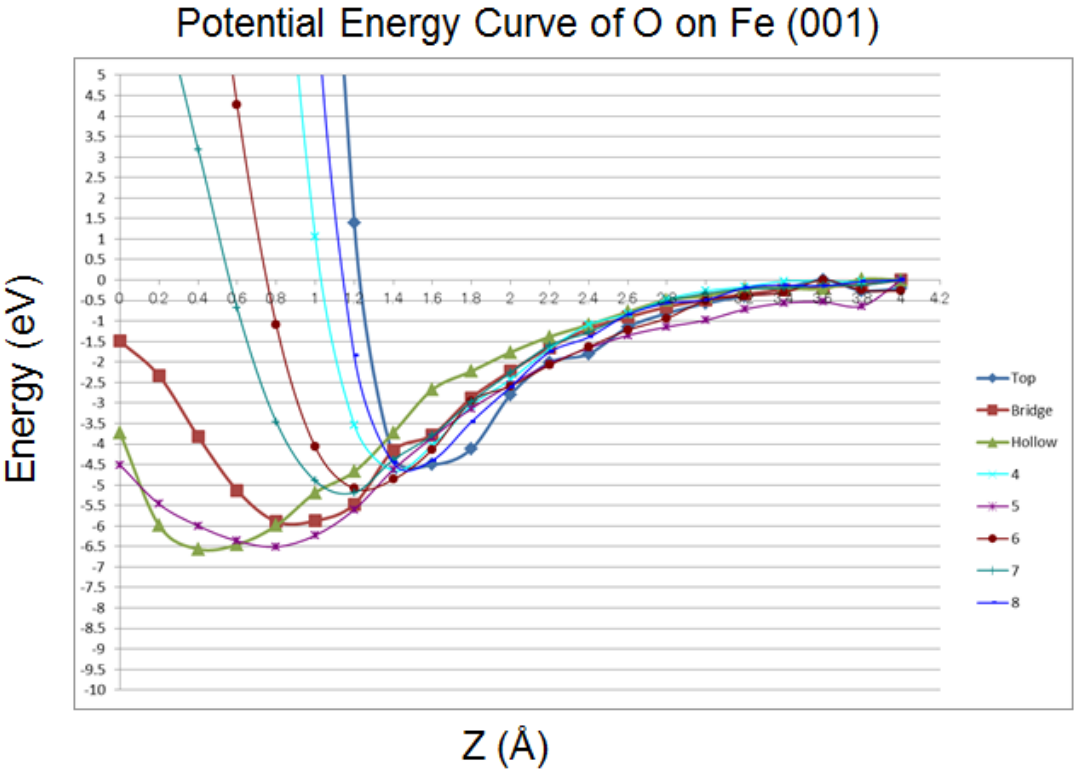

Figure 12 Potential Energy Curve of O on 5L 1x1 Iron (001)

Figure 12 shows the potential energy curve of oxygen adsorption on surface (001) of Iron. The binding site can be found also in the hollow site at a height of 0.40 Å and energy of 6.57298 eV. This height is smaller than the results of the DFT studies [4,6,8]. Charges moved from the surfaces to the oxygen atom which is the same as what happened in the adsorption of hydrogen on the surface.

In both adsorption of hydrogen and oxygen, sites near the hollow site such as 5, 6 and bridge sites show the next lower potential energies. For an OH molecule, it would be difficult for the OH to be adsorbed in iron surface if both O and H are adsorbed in the hollow site. Thus, the next lower energies would also be possible sites of binding for the OH molecule. The other part of this study covers the different orientation of OH molecule adsorption on the surface. For example, a vertical OH formation with O as frontal position as it approaches the iron surface would bind at the bridge site. This matches with the result of other DFT studies.

IV. Summary and Conclusion

This investigation is a small portion of the study on the reaction of water on Iron surface to form rusts, magnetite and then back to iron. It showed that both hydrogen and oxygen would be absorbed on the hollow site of the surface (001) of iron. The distance is about 0.40 Å above the surface of iron both for the hydrogen and oxygen. The plot of the isosurface charge difference showed that charges moved from the surface going to hydrogen or oxygen atom. These findings validated the fact that the electro negativities of hydrogen and oxygen atoms are larger than the electronegativity of iron. This information is useful for the dissociation of water to OH and H and possibility of dissociation of OH to O and H.

V. References

[1] F. Stormer, F. Wielgolaski, Environmental Science Biotechnology (2010) 9:105-107

[2] F. King, M. Kilar, Integrity Corrosion Consulting Ltd. NWMO TR-2009-07

[3] D. E. Jiang, E. A. Carter, Physical Review B **70**, 064102 (2004)

[4] P. Blonski, A. Kiejna, J Hafner Journal of Physics Condense Matter **19** (2007) 09611

[5] N R Smart, D J Blackwood, L Werme, Swedish Nuclear Fuel and Waste Management Co TR-01-22

[6] Z. Wolfram, R. Dus. Reaction, Kinetics Catalysis Letter Vol 43 No.1 231-236

[7] N.C. Debnath, A. B. Anderson, Surface Science **128** (1983) 61-69 H2O adsorption

[8] P. Blonski, A. Kiejna, J. Hafner Surface Science **590** (2005) 88-100

[9] D. J. Dwyer, S. R. Kelemen, A. Kaldor Exxon Research and Engineering (1981) H2O disso

[10] S. Lee, R. W. Staehle, Materials and Corrosion **48**, 86-94 (1997)

[11] A. Dicks, J. Power Sources **156** (2006) 108

[12] E. Lafuenta, et al. J Mater Res. **21** (2006) 2841

Experience in Japan

It was amazing that God allowed me to become a QEDC student in spite of difficulties on getting out of the country because of my government scholarship obligations and then travel to Osaka, Japan. I am happy that even though I submitted late my application, I was accepted to become part of QEDC. I am very grateful to God, to Osaka University, to Dr. Hideaki Kasai, to Dr. Wilson Diño and to the staff and researchers of Kasai lab for the opportunity they have given me to do research and be exposed to the different researches.

It was Sunday evening when I arrived in Japan. I was really thrilled and felt that I am now on my own in a different country. It was exciting and nervous since this was my first time I took the plane, be separated from my parents and to be in another country. I wondered what God has in store for me in Japan. I went out of the airport and took the limousine bus going to Umeda. Joaquin Moreno fetched me in the Umeda station and brought me to Osaka University International Students Dormitory in Satsukigaoka where I met Francisco Franco who is another Filipino. It was disappointing that my room wasn't clean but since I was really so tired I just changed my clothes and fixed my things and then went to sleep. I just cleaned my room t

The next morning I went out and saw the clean environment. Franco led me to the University. I thought the University is just near the dormitory like in the Philippines, however, it was a 1 hour walk. He brought me to the Kasai lab where no one was there at 9 am except for Eric Dona who is another Filipino who worked overnight that Sunday evening. I met the other Filipinos like Clare, Susan and Allan. I also met Kasai Sensei and Tanakan-san that morning. I realized I have many things to do like alien registration in the Suita City Hall, apply for medical insurance and open a bank account.

I studied the Vienna Ab Initio Simulation Package (VASP) alone by reading the manual, asking questions from my colleagues and trying to do the workshops and tutorial. At the same time, I did some manuscript reviews, journal readings and attended the Computational Materials Design in the Toyonaka Campus. It was two months of studying VASP and working on tungsten trioxide. Then on my third month, my study on tungsten trioxide was given to Joaquin Moreno and a study on magnetite for photocatalysis was given to me. It took me almost a month to create the complex structure of magnetite for bulk calculations. I asked for the papers from Konica Minolta and learned that I could have done first the easier part of the reaction which is water adsorption over iron surface. So I worked on the study of water adsorption on iron surface and hydrogen adsorption on magnetite surface on the fourth and last month. At the same time, I kept on reading journals and reviewed

manuscript. That was my life inside the laboratory. Outside the laboratory I met other Filipinos inside and outside the University. I met Raffy, Enzo, Paul, Joyce, Joy Rafa, Calvin, Jason, and Reg inside the University. I met Ponga, Yuri, Ptr. Lito, Stu, Frederick, and others more outside the University. I also met other foreign students in the dormitory, in the university and in the churches coming from France, Thailand, Germany, Indonesia, Malaysia, Canada, and etc. I went to some places like Osaka Castle, Farmhouse Museum, Tokyo, Kyoto and Spring8. I became part of the worship team for the Christmas Worship Service. Overall, I enjoyed my stay here in Japan. I met new friends, I got to know the culture of Japan, I was exposed to different researches in Japan.

Atmospheric-pressure plasma etching of silicon with slit aperture

Chaiyapat Tangpatjaroen, Hiroaki Nishikawa, Kohei Aida, Yasuhisa Sano and Kazuto Yamauchi

Department of Precision Science and Technology, Graduate School of Engineering, Osaka University,

2-1 Yamada-oka, Suita, Osaka 565-0871, Japan

Abstract

As a high efficient dicing process for a hard semiconductor substrate such as SiC, atmospheric pressure plasma etching with slit aperture is proposed. Basic experiments with several experimental conditions were performed using silicon wafer as a specimen. It was determined that the etching rate increases with increasing input power, SF_6 concentration and SF_6 flow rate. The maximum etching rate of 33 μm/min and the minimum etching width of 200 μm were achieved. By utilizing this process to SiC, we can also cut SiC at the etching rate of 10 μm/min with the width of 200 μm.

Keywords: atmospheric pressure plasma, plasma chemical vaporization machining, plasma etching, dicing

1. Introduction

Wafer dicing is a process by which dies are separated from a semiconductor wafer following device processing. Currently, mechanical method using diamond blade has played a key role in dicing process. The efficiency of mechanical machining method is very high, and it has contributed greatly as indispensable technology for industrial production. However, this method gives rise to the deformed layers, which means that the machined surface cannot well perform their functions [1]. Furthermore, processing efficiency of this method depends on hardness of material, which means that it is not suitable for hard semiconductor materials such as silicon carbide (SiC) or gallium nitride (GaN) expected as a next generation semiconductor substrate. Therefore, chemical etching, also called wet solving etching is a potential method. Admittedly, from the standpoint of industrial manufacturing, wet etching provides low cost and often infinite selectivity [2]. However, there is limitation in the shape of etching profile, which is undoubtedly isotropic. Dry etching, or plasma etching, is another potential method due to its great advantage on the possibility that the vertical etching rate can be exceeded the horizontal etching rate [2-4]. Indeed, the dry etching technique has become more important in fabrication of semiconductor because it is required precision and damage free control in order to produce high-performance electronic devices.

However, conventional plasma etching usually

processes in low pressure environment. Because, the plasma generated by this method has long mean free path and low radical density, the processed surface can be damaged and the etching rate is very low. It is not suitable for a process which needs a large amount of removal, such as dicing process. Thus, atmospheric-pressure plasma etching [5-8] which has a property of high removal rate seems to be the most potential method to dice a hard semiconductor wafer such as SiC or GaN. Figure 1 shows a concept of dicing using line plasmas. The first attempt to apply atmospheric pressure in plasma process is to use atmospheric pressure plasma with a wire electrode. However, when the wire electrode is being used with increasing SF_6 concentration to get higher depth, it is necessary to increase power too. As a result, the wire electrode was broken due to the excessive thermal stress and could not achieve enough removal rate. Therefore, we propose the new method that to use a bulk electrode and a slit aperture in order to generate a line plasma with higher thermal resistance. In this report, results of basic experiments of etching of silicon using on atmospheric - pressure plasma with slit aperture and a trial experiment of etching of SiC are described.

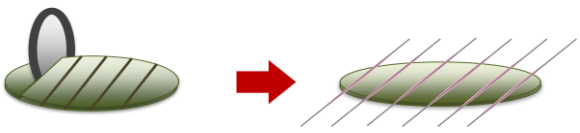

Fig. 1. Concept of dicing using line plasma

2. Concepts of plasma etching

2.1 General concepts

Plasma etching is one of the basic techniques used in semiconductor processing for the fabrication of electronic devices. In a low pressure environment, plasma is produced by the dissipation of electrical power to the reactant. Electron gains most of the transfer energy, which has enough power to initiate processes such as dissociation, ionization and excitation. Atoms, radicals and ion species, which are produced in this way, are now being collected together into clusters. Therefore, the plasma phase is generally a very complex mixture of many chemical species.

In reality, the inlet gas is consumed and the need for a gas flow to replenish the consumption is apparent. Then, the reactant gas has to be continuously fed and maintained the low pressure by pumping of vacuum system. The choice of the gas mixture depends on the volatility and stability of the etch product. For element materials, such as Si, the choice is generally easy and large since several alternatives exist such as CF_4 or SF_6, which allow to use in the etching process efficiently [9,10]. After the plasma was generated, these gases can produce chemically active species which can react with the substrate as shown in Fig 2.

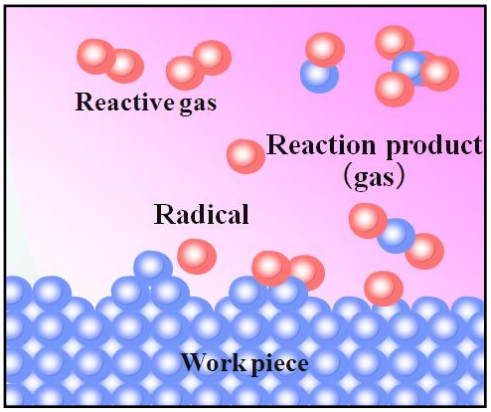

Fig. 2. Plasma and material interaction

2.2 Atmospheric-pressure plasma etching

For many years, conventional plasma etching has been proved to be useful method. However, there are still some drawbacks which are low etching rate and broad plasma around electrode. In recently, atmospheric-pressure plasma etching or PCVM (Plasma Chemical Vaporization Machining) was developed to solve these problems. In PCVM, the plasma was generated under high pressure environment in order to get high concentration of radicals which leads to higher etching rate compare to conventional plasma etching. Moreover, the mean free path obviously decreases at higher pressure and ultimately resulting in very low ion energy which can create no damage on the surface. Not only the high pressure environment affects ion energy, it also allows the localization of plasma around electrode and the concentration of power equal to that of mechanical removal can be obtained in the process.

3. Experimental Procedure

The substrate used in this work was Si (001) and SiC. This substrate was set in the chamber as shown in Fig. 3. To investigate the etching characteristic, various types of aluminium electrodes have been utilized as shown in Fig. 4. and the machining procedure using this device is as follows. First, the slit aperture is set between specimen and the electrode with desired gap width. Then, the chamber was evacuated and filled with mixing gas of He and SF_6 at one atmospheric pressure. By applying power and flowing both of He and SF_6 as reactive gases at the center of electrode, plasma was generated in the gap area. Experimental conditions are shown in Table 1.

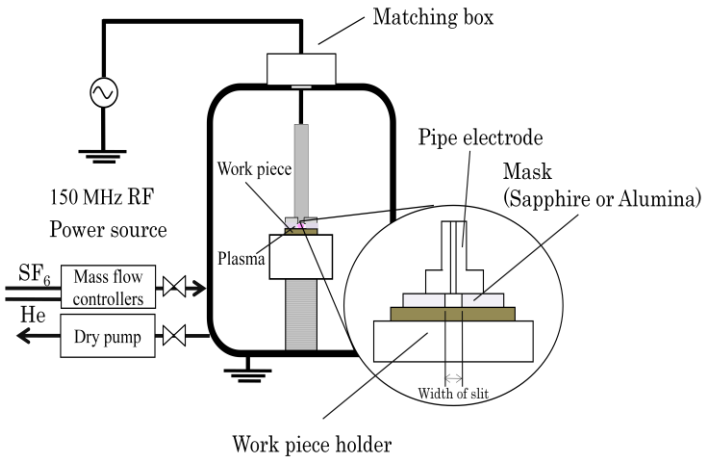

Fig. 3. Schematic of new PCVM apparatus

Table 1. Experimental condition in various experiments

	I	II	III	IV	V
Process gas (%SF_6)	0.20%	0.40%	0.40 - 0.80 %	1.00%	1.00%
Input power (Watt)	50	60 - 150	150	150	150
Gas flow rate (sccm)	30	30	30	10 - 80	60
Width of slit (μm)	400	400	400	200	100 - 200
Mask thickness (μm)	400	400	400	185	185
Time (min)	5 - 60	10	10	5	5
Electrode	A	A	A	B	B

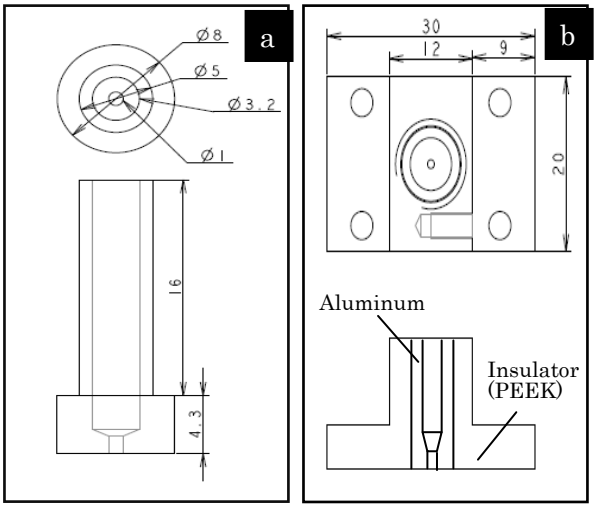

Fig. 4. Electrodes

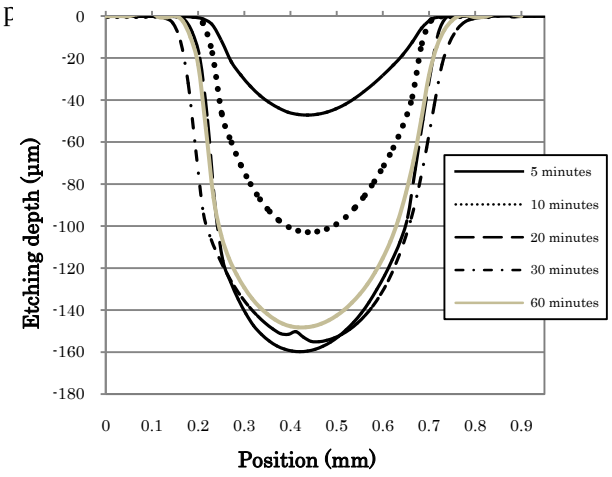

Fig. 5. Effect of machining time on etching profile

After processing, the cross-sectional shape was measured using a stylus surface profiler. The etching rate was determined from the etched depth and compare with other parameters.

4. Results and Discussion

4.1 Machining time effect

The relationship between etching depth and etching time was examined in condition I shown in Table 1 and the result was shown in Fig. 5. In atmospheric pressure plasma etching of Si, it was observed that the etching depth is increasing with machining time from 5 to 60 minutes. Nevertheless, the result shows that this trend seems to have limitation. The maximum etching depth may be depends on the distance between electrode and specimen.

4.2 Input power effect

The relationship between the etching depth and input power was examined in condition II shown in Table 1and the result was shown in Fig. 6. In each input power conditions, an increase in input power

Input power from the source must be high enough to ignite the discharge and has sufficient power to get enough the number of reactive radicals. However, in this experiment, the impedance matching circuit has not been used while generating plasma to compensate power loss.

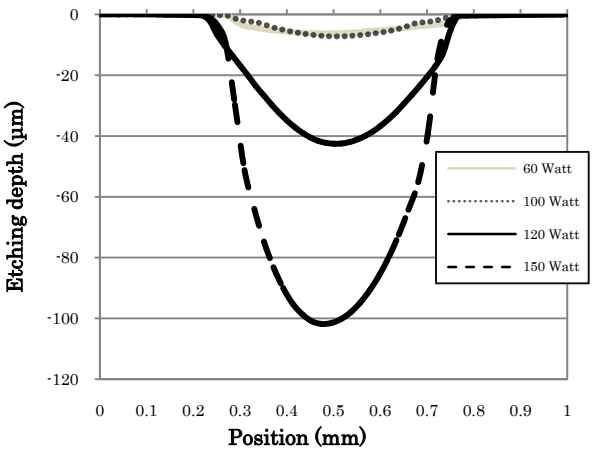

Fig. 6. Effect of input power on etching profile

4.3 SF_6 concentration effect

After using matching box while plasma was generated, the etching depth gets deeper. For example, at 0.4% and 150 Watt, the etching depth is

increased from approximately 100 μm as shown in Fig. 6 to 200 μm. in Fig. 7. The relationship between the etching depth and SF_6 concentration was examined in condition III shown in Table 1 and the result was shown in Fig. 6. Then, the investigation of SF_6 concentration effect was carried out. The effect of SF_6 concentration was shown in Fig. 7. These graphs show that the etching depth gets deeper with increasing SF_6 concentration from 0.4% to 0.7%. However, in the 0.8% condition, the plasma was barely generated. So, the specimen can be etched only 108 um in depth. The dependence of etching depth on SF_6 concentration seems clear but, it is seen from the graph that it has asymmetric depth profile. There are two possible reasons for this matter. First, the face of electrode and the masks are not parallel. The second, the gas inlet is not in the center of the mask gap. Then we design a new electrode to use in PCVM apparatus as shown in Fig. 4(b).

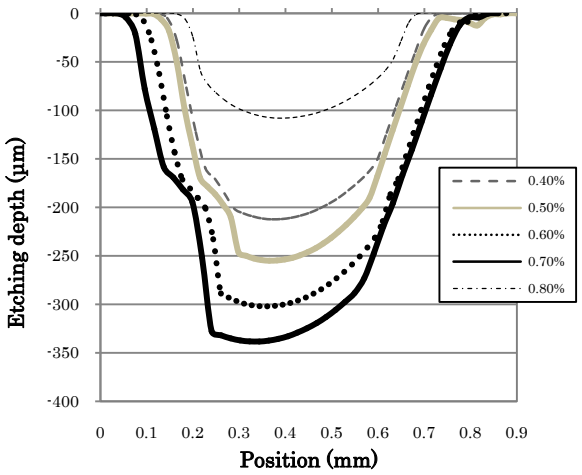

Fig. 7. Effect of SF_6 concentration on etching profile

4.4 SF_6 flow rate

The relation between the etching depth and SF_6 was examined (condition IV shown in Table 1) and the result was shown in Fig. 8. The purpose of this section is to investigate the dependence of etching profile upon SF_6 flow rate. The results show that when SF_6 flow rate is increased, the etching depth is increasing as shown in Fig. 8. The reason for this behavior is maybe due to an inadequate supply of reactant gas. If using higher gas flow rate, the more supply of reactant gas and the more radical generated which ultimately resulting in deeper etching profile.

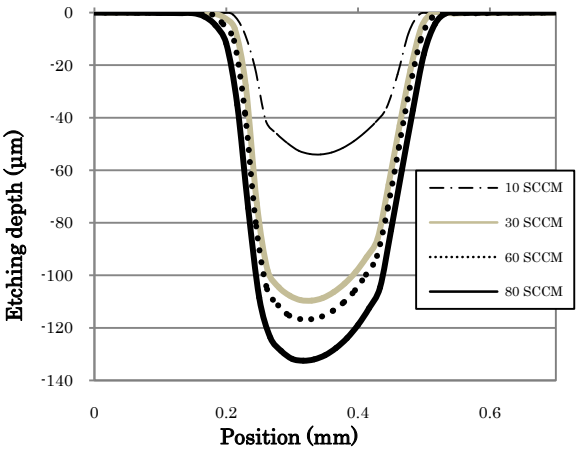

Fig. 8. Effect of SF_6 flow rate on etching profile

4.5 The width of slit effect

The relation between the etching depth and slit effect was examined (condition V shown in Table 1) and the result was shown in Fig. 9. The last parameter is the width of slit. We found that the etching depth is higher when the width of slit is wider. However, we have not been able to conclude this result yet, because we found later that there is gas leak in the gas tube due to overpressure in 100 um slit case.

4.6 The shape of etching profile

From many last sections, we consider only

etching depth characteristic. But now we will consider the shape of etching profile. As shown in Fig. 5 and Fig. 10, although the etching depth profile has undercut, the shape is like anisotropy. If you consider etching rate, in the most cases, the etching rate in vertical direction is higher than horizontal direction.

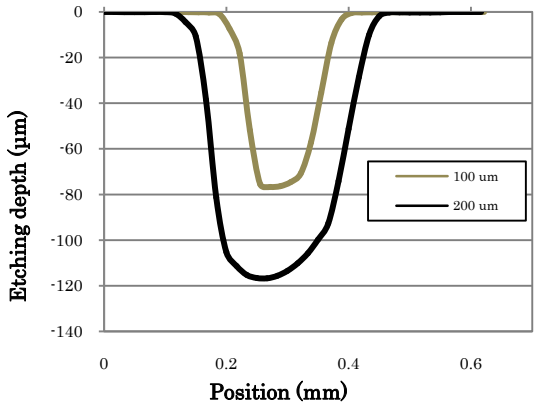

Fig. 9. Effect of width of slit on etching profile

For example, in machining time effect investigation, all of etching rate in the vertical directions are higher than horizontal directions as shown in Fig. 10. This phenomenon is believed to be the result of non-uniformity of plasma or the inactivation of reactive species at the sidewall of the slits.

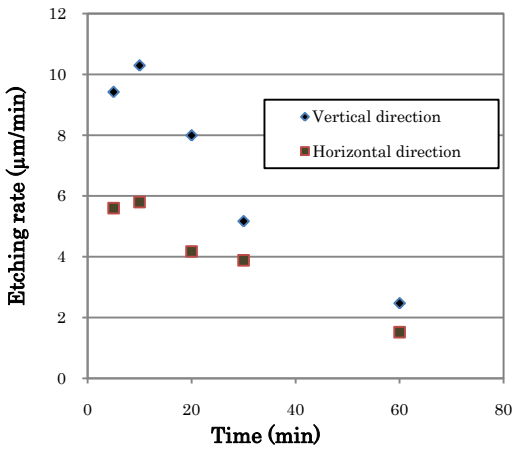

Fig. 10. Effect of time on etching rate

4.7 Dicing of SiC

The first trial of dicing of SiC with slit aperture was performed by the same method of Si with the power of 150 Watt for 10.45 minutes. The gas flow rate was 30 sccm and the SF_6 concentration was 1.0%. With the use of 185 μm mask, the result of experiment shows that the etching rate of SiC can be reached at approximately 10 μm/min as shown in Fig. 11. Comparing to wire electrode case, it is seen that this method has much more etching rate and the width is shorter. Moreover, it has almost the same dicing behavior like in Si cases. So, this process has possibility to cut SiC.

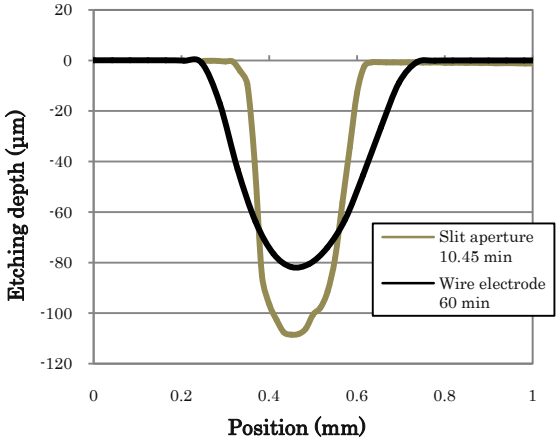

Fig. 11. Comparison of the two methods in dicing SiC

5. Conclusions

An atmospheric-pressure plasma etching with slit aperture was proposed as a novel dicing technique. Basic experiments were performed using a Si wafer. The etching depth profile and the etching rate depend on the process parameters. The following conclusions in process parameters can be reached based on the above result:

1. In the machining time effect, the etching

depth is higher when the machining time is increasing.

2. As for SF_6 concentration, the etching depth is increasing with SF_6 concentration until reach maximum limit at each input power.
3. For input power factor, the etching depth increases with input power.
4. As for gas flow rate parameter, when SF_6 flow rate is higher, the etching depth gets deeper.
5. The last parameter is the width of slit. It was found that when the width of slit is lower, the etching width is lower.

From these experiments, the maximum etching rate of Si was 33 μm/min and the minimum etching width was 200 μm. They are quite higher and narrow compared with the experiment with wire electrode and attain to the level of practical use. Also, it was found that a SiC wafer could be cutted at the rate of 10 μm/min with the width of 200 μm, that could never be achieved by atmospheric - pressure plasma etching with wire electrode.

Acknowledgements

We are thankful for the support from Quantum engineering design short term program scholarship and Osaka University.

References

1. Y. Mori, K. Yamamura, K. Endo, K. Yamauchi, K. Yasutake, H. Goto, H. Kakiuchi, Y. Sano, H. Mimura: Journal of Crystal Growth 275 (2005) pp. 39-50.

2. H. Kamimura, R. J. Nicholas and R. H. Williams, Plasma etching: fundamentals and applications, Oxford University Press Inc., New York (1998).

3. Ch. Cardinaud, M.-C. Peignon, P.-Y. Tessier, Applied Surface Science 164 (2000) 72-83.

4. B. Chapman, *Glow discharge processes: sputtering and plasma etching*, John Wiley & Sons, Inc., Canada (1980).

5. Y. Sano, M. Watanabe, K. Yamamura, K. Yamauchi, T. Ishida, K. Arima, A. Kubota and Y. Mori: Japanese Journal of Applied Physics Vol. 45, No. 10B (2006), pp. 8277-8280.

6. H. Takino, N. Shibata, H. Itoh, T. Kobayashi, H. Tanaka, M. Ebi, K. Yamamura, Y. Sano and Y. Mori: Jpn. J. Appl. Phys. Vol. 37 (1998) pp. L894-L896.

7. Y. Mori, K. Yamamura, K. Yamauchi, K. Yoshii, T. Kataoka, K. Endo, K. Inagaki and H. Kakiuchi: Nanotechnology 4 (1993) 225-229.

8. H. Takino, N. Shibata, H. Itoh, T. Kobayashi, H. Tanaka, M. Ebi, K. Yamamura, Y. Sano and Y. Mori: Applied Optics Vol. 37 No. 22 (1998) pp. 5198-5210.

9. R. W. Liptak, B. Devetter, J. H. Thomas III, U. Kortshagen and S. A. Campbell: Nanotechnology 20 (2009) 035603 (5pp).

10. K. M. Eisele: J. Electrochem. Soc.: Solid-State Science and Technology Vol 28. No. 1 (1981) pp. 123-126.

My Life as a short term student in Osaka University

I think I got interested in Japan even before I got this wonderful opportunity to participate in QED short term program and, admittedly, it was one of the most unforgettable experiences of my life. I have only been in Japan for five months but the life of study in Japan is full of everything. Sometimes it is "happy", sometimes it is "nervous", sometimes it is "exciting", and most of the time it is "difficult", but it's meaningful, fruitful and colorful more than I first expected.

Figure 1: Me in Kyoto

On the first day in Japan, I was picked up by two of my lab mates at Itami airport, and then they took me to my dormitory and Suita city hall to complete my documents and move-in procedures. After that, they took me to Yamauchi lab to meet my project advisor. He was very welcome and he introduced me about Yamauchi laboratory. After that I was collected by some Thai people here who came to study before me in order to introduce me with other Thai people here in Japan. After that, they gave me a mobile phone and a new bicycle to use in the next five months. On the following days of the week, I finally met my very nice advisor. On my first meeting with my new advisor we chatted for quite a while and he took me to introduce with my tutor, Mr. Aida, and after that he took me to the ultra cleaning room, the place where my most experiments would take place and showed me how to operate the machine.

At the end of the day, all Yamauchi laboratory members held welcome party for me at Sushi shop. That is the first time I ate sushi in Japan and it is very delicious. Of course, maybe except Natto sushi, it has very unique taste to my tongue but you must try it. My life here is challenging at times, but it is also very rewarding. My ability to communicate has been limited, but the kind friends and professors here at Handai make it possible for me to feel welcome and understood. Their gestures were quite touching and it made me comfortable with research work and very happy too.

Admittedly, although I have invaluable assistance from my advisors and others in Yamauchi laboratory, it still took me about two weeks to adapt myself to Japanese lifestyle. Perhaps, I got my first culture shock for the first time when I went shopping. I realized that I could neither read the letters nor recognize most of the things displayed on the shelves. I spent several days trying to experiment with the few recognizable ones and not surprisingly, I made lots of mistakes. I ordered Remen thinking it was

Ramen, bought yogurt and thought it was milk. It was also difficult to adjust to Japanese lifestyle such as, the different procedures of transportation, waste management and climate change preparation, but I guess it was part of new things to learn and adjust to.

However, the food here was amazing! I'm someone who has more experience in trying a new food, especially strange things and while I am in Japan I wanted to have the full experience, so I forced myself to try everything, and they were actually delicious. Japanese ramen is mouth-watering, and if you get the chance a traditional Japanese restaurant, it is a very interesting experience. I would definitely recommend Sushi, Takoyaki and Okonomiyaki, as well as Shabushabu and Sukiyaki although the Japanese make excellent treats and cakes, so I guarantee you won't go hungry in Japan!

As the time was going by, the weather is changing, because I came here at the season changes from summer to autumn. The trips which summer I went such as Kyoto and Nara to Wakayama in the autumn are very nice and beautiful. Moreover, I had a chance to join Yamauchi laboratory trip, Gero-onsen and Shirakawago trip, which is very good. In these two trips, I have an opportunity to drink Sake and taking a bath in onsen. I found that Ume-sake is very delicious and I feel very relax when I was being in onsen.

Figure 2: Yamauchi Laboratory member

Apart from sightseeing and experiencing Japanese culture, most of the time I do my research with my tutor, Aida ,and my buddy, Hiro. Moreover, I often have opportunity to go to many workshops, conferences and exhibitions. For example, I attended CMD17 workshop at Toyonaka Campus on early September, Cheiron school in the middle of October and SEMICON Japan 2010 in the first days of December. Though, most of lectures are in Japanese but the workshop is very useful and provided me with wide perspective in another field.

On my last week, my friends took me to one of Japanese restaurant and performed something for me. It was one of the most magical things I have ever seen. I knew that I would never forget it, and I will think of about Osaka, my friends and all the people I have met every day during 5 months. The trip did wonders for my study and Japan is one of those countries where you have to live the culture in order to

fully appreciate and understand it. I will miss Osaka a lot and I hope to return there someday, and I'm so happy I got the opportunity to be here. I will always have this wonderful experience in my mind!

Study on Removal Mechanism of Catalyst-Referred Etching on 4H-SiC (0001) Surface

Bui Van Pho, Shun Sadakuni, Takesi Okamoto, Yasuhisa Sano, and Kazuto Yamauchi

Department of Precision Science and Technology, Graduate School of Engineering, Osaka University

2-1 Yamaoka, Suita, Osaka, Japan

Abstract

A novel abrasive-free planarization method called catalyst-referred etching (CARE) has been developed. In this method, we use platinum as a catalyst and hydrofluoric acid as an etchant. After the CARE process, a flat and well-ordered surface has been observed by atomic force microscopy (AFM). To understand the atomic structure at the topmost surface, we observed high-resolution transmission electron microscopy (HRTEM) images of a 4H-SiC (0001) wafer by using a standard commercial 2-inch n-type 4H-SiC (0001) wafer cut 8 degrees off-axis toward the $[1\bar{1}00]$ direction.

Introduction

Silicon carbide is a semiconductor material having a number of polytypes such as 4H and 6H-SiC. The crystal structure in the $[11\bar{2}0]$ direction of 4H and 6H-SiC are 4 bilayers and 6 bilayers, respectively. The alternating of HCP and FCC structures of both 4H and 6H-SiC are clearly shown in Figure 1. In the case of 4H-SiC, the alternation is 1 bilayer of HCP with 1 bilayer of FCC. Moreover, in the case of 6H-SiC, the alternation is 1 bilayer of HCP with 2 bilayers of FCC.

Silicon carbide (SiC) has recently gained much attention due to its excellent electrical, thermal, and mechanical properties. In particular, SiC is a promising material in high performance devices such as high power, high temperature, and high frequency devices. SiC surfaces for these applications require good flatness, low micro-roughness, and a crystallographic non-damaged surface. However, such SiC surface is difficult to obtain because of the extremely hardness and chemical inertness of the SiC materials. Fortunately, a novel abrasive-free planarization method, which is called catalyst-referred etching (CARE), has been developed [1]. Highly crystallographic ordered surface can be formed with an atomic step-and-terrace structure.

In the CARE process, chemical etching is induced preferentially at the pump areas on the surface because the areas are selectively in contact with the catalyst plate. The plate has a planar surface, which plays a similar role as the polishing pad for CMP (chemical mechanical polishing).

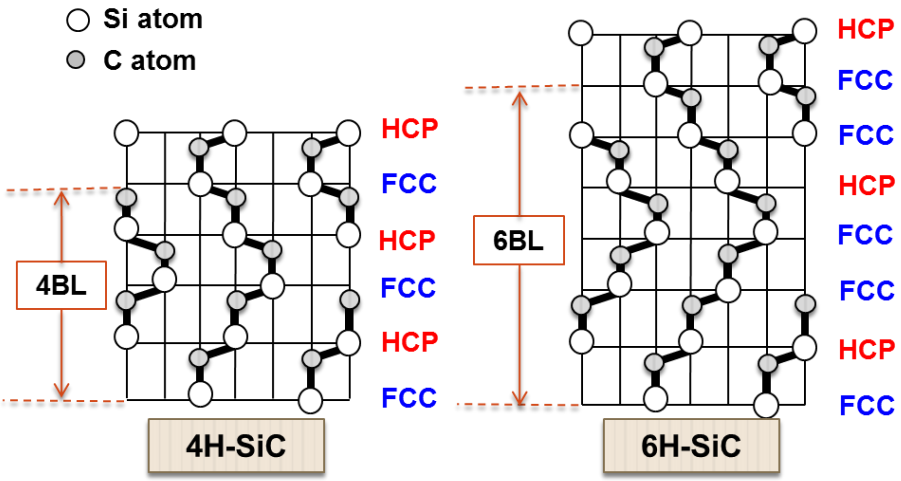

Figure 1: Crystal structures of 4H-SiC and 6H-SiC in the $[11\bar{2}0]$ direction.

In the case of SiC CARE, platinum (Pt) is used as a catalyst plate and hydrofluoric acid (HF) is used as an etchant. The schematic diagram of SiC CARE system is shown in Figure 2. It has been reported that the topmost atoms of the SiC surface are preferentially removed through an electron transfer between the SiC and the Pt catalyst [2]. The flat surface with root-mean-square (RMS) roughness of less than 0.1 nm can be obtained by CARE. Especially, the CARE-processed SiC surface is flat and non-damaged over the whole wafer [3].

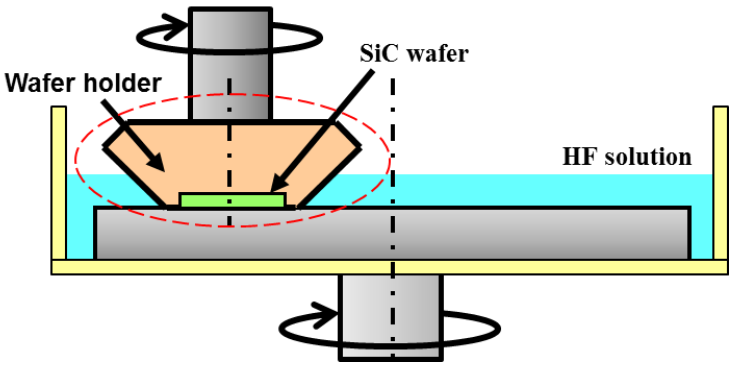

Figure 2: The schematic of SiC CARE system.

In experiments, the step-and-terrace structure with alternating wide and narrow terraces, straight step edges, and a 0.25 nm single bilayer step height was observed after CARE, along the $[1\bar{1}00]$ direction, on a 4H-SiC (0001) wafer surface cut 8 degrees off-axis toward the $[11\bar{2}0]$ direction [4]. The relationship between the alternating hexagonal close-packed (HCP), face-centered cubic (FCC) structures and wide, narrow terraces is not yet well understood because of the similarity in the atomic configurations of the HCP and FCC of the 4H-SiC surface in the $[1\bar{1}00]$ observing direction. Thus, in this study, to clarify this relationship, a detailed characterization of the CARE-processed surface structures has been performed by

using HRTEM observation, along the $[11\bar{2}0]$ direction, of the CARE-processed 4H-SiC (0001) surface 8 degrees off-axis toward the $[1\bar{1}00]$ direction.

Experimental details

In this study, we use a standard commercial 2-inch n-type 4H-SiC (0001) wafer, which is cut 8 degrees off-axis toward the $[1\bar{1}00]$ direction. The wafer is put on the platinum plate for CARE planarization process, at the pressure of 400 hPa. Both the wafer and the plate are immersed in 25 mol/l hydrofluoric acid solution, and independently rotated at speeds of 10.0 and 10.1 rpm in the same direction, respectively. The wafer is planarized for 3 hours with the removal rate of 60 nm/h, and then verified for the surface roughness by atomic force microscopy (AFM, SII Nanotechnology, Inc. Chiba, Japan, SPA400 + SPI3800N). Then, the wafer is coated by carbon for surface protection, as shown in figure 3a.

The TEM sample is prepared by using the focused ion beam (FIB 2100) micro sampling technique, as shown in figure 3b. The sample is thinned down to 70 nm and then polished by argon ion milling system (0.3–1 kV, Gentle Mill IV5; Technolog Linda. Ltd, Hungary). The sample is observed along the $[11\bar{2}0]$ direction with accelerating voltage of 200 kV (JEOL JEM-2100, LaB6). In this observing direction, each column consists of the same chemical element, being either silicon or carbon (figure 1).

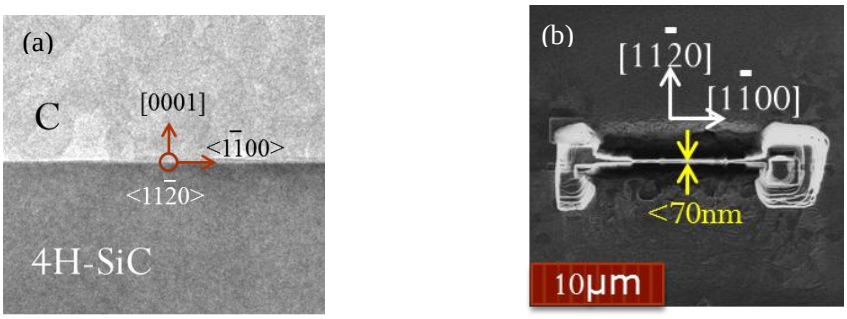

Figure 3: (a) a TEM sample with carbon protective layer in the $[11\bar{2}0]$ direction.
(b) A TEM sample was prepared by FIB.

Results and discussion

2μm x 2μm AFM images of planarized surfaces of a 8 degrees off-axis-cut 4H-SiC (0001) wafer, an on-axis 4H-SiC (0001) wafer, and an on-axis 6H-SiC (0001) wafer are shown in figures 4a, 4b and 4c, respectively. The RMS roughness of the CARE-processed surfaces is less than 0.1 nm. The step-and-terrace structure with regularly alternating of wide and narrow flatten terraces can be observed after CARE in the case of the on-axis wafers (figures 4b and 4c). The step-and-terrace structure, in the case of 8 degrees off-axis wafer surface, cannot be observed by AFM due to the high step density and the spatial resolution limit of AFM.

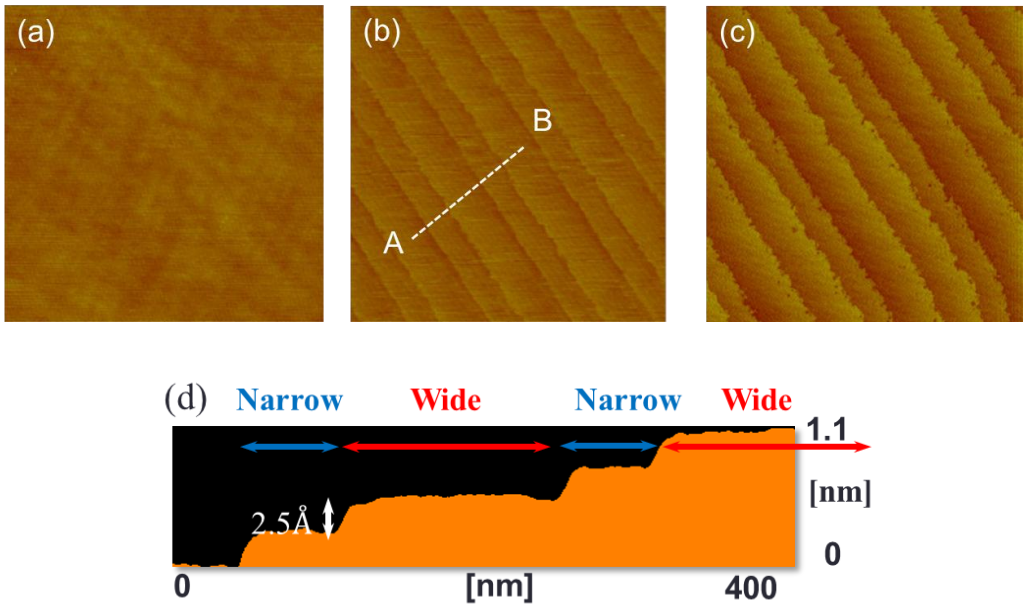

Figure 4**:** 2µm x 2µm AFM images of planarized surface of (a) a 8 degrees off-axis-cut 4H-SiC (0001) wafer, (b) an on-axis 4H-SiC (0001) wafer, and (c) an on-axis 6H-SiC (0001) wafer. The RMS is less than 0.1 nm. (d) The cross-section cut from A to B in (b).

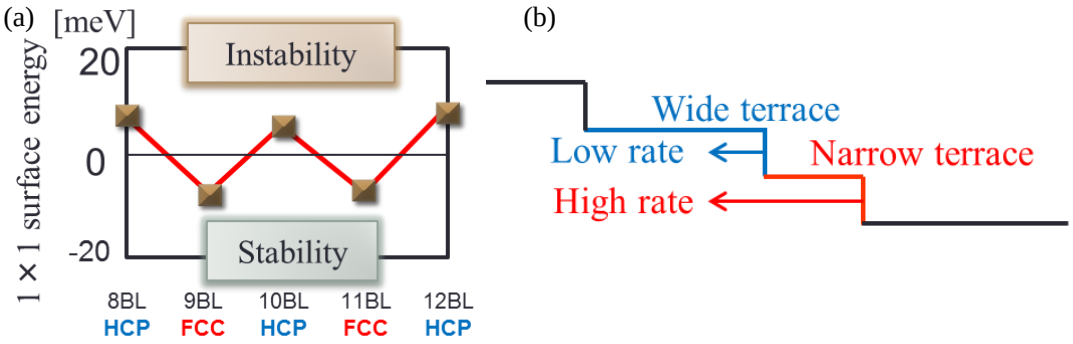

Figure 5: (a) Stability of HCP and FCC. (b) The formation mechanism of wide and narrow terraces

Figure 4b shows the regularly alternating of 1 wide and 1 narrow terraces of the on-axis 4H-SiC (0001) wafer surface. Moreover, in the case of the on-axis 6H-SiC (0001) wafer surface, the regular alternation is 2 wide and 1 narrow terraces. The alternations of HCP and FCC in the crystal structures of 4H and 6H-SiC are the same as that of wide and narrow terraces in the AFM images of 4H and 6H-SiC. Therefore, the alternating of HCP and FCC structures of 4H-SiC wafer is considered to be related to the alternating wide and narrow terraces observed after CARE. The characteristic width of terraces with 1 bilayer step height has been observed in the both cases. From these results, we suggest that the removal process in CARE occurs only at the step edges of topmost surfaces and the wide terraces are considered to be FCC.

The surface energy of HCP and FCC has been performed using density functional theory calculations [5]. This study confirmed that FCC surface energy is smaller than that of HCP. It means that

FCC surface is more stable than HCP surface. The stability of HCP and FCC is demonstrated in figure 5a. We suggest that the difference in etching speeds at the step edges of the topmost surfaces because of the energy difference of HCP and FCC surfaces leads to the formation of wide and narrow terraces, as demonstrated in figure 5b.

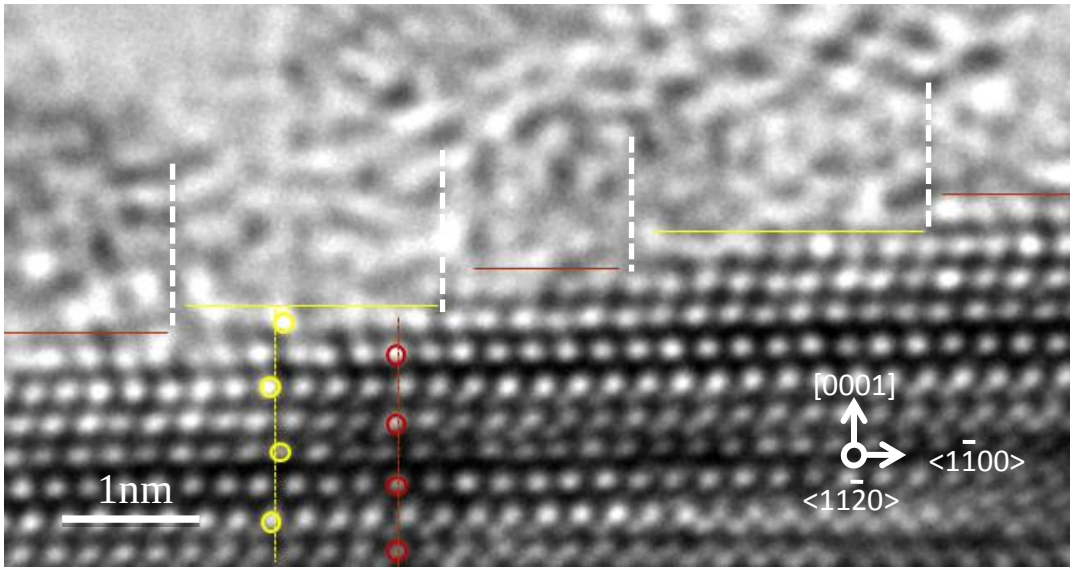

Figure 6: HRTEM image along the $[11\bar{2}0]$ direction of 8 degrees off-axis-cut wafer (Magnification of 1,200,000).

To confirm the relationship between the terrace widths and the atomic structures in more details, we observe the CARE-processed surface with a HRTEM. An obtained image of the 4H-SiC wafer surface taken along $[11\bar{2}0]$ direction is shown in figure 6. In this image, contrast transfer function (CTF) is positive and therefore it produces a negative phase contrast, means white atoms. The white spots in this image are silicon (Si) atoms. The contrast of image varies depending on specimen thickness and defocus. The darkness increases with increasing the thickness. The image becomes rather complicated in the thicker region of the sample.

The positions of the Si atoms in vertical columns (in the [0001] direction) of HCP is in straight lines for all bilayers in contrast with that of FCC, the alternating of positions of Si atoms in vertical directions of FCC (fig. 1). Hence, we can easily clarify the terraces structure base on the positions of Si atoms in the HRTEM image. From figures 1 and 6, we can easily estimate the wide terraces are FCC and the narrow terraces are HCP. These results are also coincided with molecular dynamics calculations which are showed the energy difference between HCP and FCC surfaces [5].

Summary

The flat and well-ordered with the alternating of wide and narrow terraces of 4H-SiC and 6H-SiC CARE-processed surfaces have been obtained and confirmed by AFM and HRTEM images. The surfaces can be obtained because the etching mechanism of CARE occurs at only the step edges of the topmost surfaces. The regularly alternating of wide and narrow terraces is formed because of the difference between the removal speeds of HCP and FCC surface structures. HRTEM observation of 4H-SiC (0001) wafer surfaces have confirmed that wide terraces are FCC and narrow terraces are HCP.

Acknowledgements

This work was supported by Quantum Engineering Design Short-Term Program, Osaka University, Japan. Sample preparation with low energy ion beam milling was supported by Prof. Eiji Taguchi at Research Center for ultra-high vacuum electron microscopy (Ultra-HVEM), Osaka University.

References

[1] H. Hara, Y. Sano, H. Mimura, K. Arima, A. Kubota, K Yagi, J. Murata, and K. Yamauchi, Novel abrasive-free planarization of 4H-SiC (0001) using catalyst, J. Electron. Mater. **35** (2006) 8.

[2] K. Arima, H. Hara, and J. Murata, Atomic-scale flattening of SiC surfaces by electroless chemical etching in HF solution with Pt catalyst, Appl. Phys. Lett. **90**, (2007) 202106.

[3] T. Okamoto, Y. Sano, K. Tachibana, K. Arima, A. N. Hattori, K. Yagi, J. Murata, S. Sadakuni, and K. Yamauchi, Dependence of process characteristics on atomic-step density in catalyst-referred etching of 4H-SiC (0001) surface, J. Nanosci. Nanotechnol. **11** (2011) 2928–2930.

[4] S. Sadakuni, N. X. Dai, Y. Sano, K. Arima, K. Yagi, J. Murata, T. Okamoto, K. Tachibana, and K. Yamauchi, TEM observation of 8 deg off-axis 4H-SiC (0001) surfaces planarized by catalyst-referred etching, Mater. Sci. Forum **679-680** (2011) 489-492.

[5] H. Hara, Y. Morikawa, Y. Sano, and K. Yamauchi, Termination dependence of surface stacking at 4H-SiC (0001)-1x1: Density functional theory calculations, Phys. Rev. B **79**, (2009) 153306.

Osaka University

Graduate school of Engineering

Quantum Engineering Design Short-Term Program

Research student: Bui Van Pho – 1 year course

Life as a short term student in Osaka University

My name is Bui Van Pho. I am a research student from Vietnam. I knew the Quantum Engineering Design (QED) Short-Term Program when I studied at undergraduate school, College of Science, Vietnam National University – Hanoi. My last supervisor introduced me to this program. At that time I felt so excited and would like to be come a student in this course. Fortunately, I have been selected to be a short-term research student for one year.

I came to Japan in October 2010. As a newcomer, I was still at a loss about everything. With the help of my lab mates and Quantum Engineering Design staffs I could easily adjust with my new life.

Figure 1: Taken with professors and students in Quantum Engineering Design Course at the party in Computational Materials Design Workshop - March 2011

When I was a research student in Osaka University, I studied how to deal with a problem independently in both research activities and daily life. I had chances to study and use modern machines to approach to modern, up-to-date techniques related to advanced quantum engineering design in response to global technological and environmental issues. When I had some difficulties I could have a discussion with my tutor and my supervisor. They were always ready for helping and supporting me. Furthermore, I could have a chance to attend the lectures and the 18th Computational Materials Design (CMD) Workshop related to my research and study. I had good relationships with teachers and other QED students coming from various countries. The picture, which is shown in figure 1, was taken with QED teachers and students at the party in the 18th CMD Workshop.

The study environment in Osaka University is excellent. I have never studied in such a professional study environment as Osaka University. In addition, I also took part in Japanese language classes. It is really necessary for me, when I am here, in Japan, especially in the future for the global corporation.

In daily life, I lived in the dormitory of Osaka University in Suita campus. With a fully equipped room and friendly neighbors, it is a great place for living and studying. Although Osaka University is located in rural areas, there are many trains and subways for transportation to go to the center or to other places. Osaka is part of Kansai region, which is very beautiful and has a long and rich history. It is very easy and comfortable to travel to beautiful and traditional places, such as shrines, temples, towers, castles… in Kyoto, Nara, Hyogo, and Osaka prefectures. Furthermore, Japan is an ordered and peaceful society. I always felt so secure and peaceful when I went out, even at midnight. I am very enjoying my life here.

Figure 2: Taken with Japanese friends from Wakayama University at the Hanami party at Osaka Castle.

There are many traditional festivals in Kansai. I often enjoyed my weekends, after finishing studying in weekdays, with my friends – both Vietnamese and Japanese. For example, we took part in the hanami (means cherry blossoms viewing) parties with Japanese friends at Osaka castle and with my lab members at Osaka University, as shown in figure 2. Japanese are very kind and polite. I love Japanese people and love Japan.

After one year study, I got a lot of knowledge and experiences in both scientific and daily life. Without the useful advises from QED staffs and my supervisor, I cannot succeed in both my research and comfortable life in Japan. This course brings me a lot of opportunities and challenges for my future carrier and research. Fortunately, I have passed the entrance examination to continue my study here, in Quantum Engineering Design Course, Master course. My story is continuing and I will have a lot of chances to enjoy my life in Japan.

Finally, I would like to say “thank you very much” to Quantum Engineering Design staffs, my supervisor and Japanese friends for your help during the last year. I highly appreciate it.

Reactivity of Dissociative Adsorption of O_2 on Cu and Pt surfaces

CicaGustiani

Abstract

In this study, the effect of surface structure and constituent atoms on the reactivity of surfaces are analyzed by comparing the dissociation of O_2 on clean (001) and (111) surfaces of Cu and Pt using first principle calculations within density functional theory (DFT). The reactive pathways are derived from the trace of energy minimum under the same conditions. Results show that the difference in O_2 dissociative adsorption on the different surface structures is given by the quasiatomic adsorption on (111) and dissociative adsorption on (001) surface. The quasiatomic adsorption on (111) surface is due to the local structure of the surface. Also, changing the surface structure affects the surface reactivity of O_2 dissociative adsorption. Here, (001) surface is more reactive than (111) surface because of the lower activation barrier and higher adsorption energy at the former than the latter. The difference in O_2 dissociative adsorption for different constituent atoms is given mainly by adsorption which is mediated by precursor states on Cu and direct dissociation on Pt.

1. Introduction

Surface science has a very important role in the development of myriad technologies which are crucial for energy and environment either now or in the future. Fields of applications that involve chemical reactions at surfaces, especially on metal surfaces, are incredibly large. Some examples include semiconductor processing, corrosion, electrochemistry, and heterogeneous catalysts. Heterogeneous catalyst itself has been estimated to be a prerequisite for more than 20% of all production in the industrial world [1] and potentially growing in years to come.

Oxygen Reduction Reaction (ORR) is one of the most studied, not only because it is interesting scientifically but also because of its importance in various practical purposes. To give an important example, ORR occurs on catalyst in the cathode of fuel cells which nowadays typically uses platinum (Pt) based catalysts. However, Pt is still a rare material on Earth. In addition, there is a long term need to provide solutions to the energy problems to identify more sustainable power sources for now and the future. In other hand, oxidation on copper (Cu) is an interesting process. Corrosion on it can be seen in our daily lives. This is described by some interaction between oxygen and Cu. This in turn, represents an important process which can be promoted or prevented, depending on how Cu is used [2].

In designing catalytic materials for certain reaction, it is important to know the properties that can be used to control surface reactivity. To achieve this, it is important to identify the key properties that can be used as control parameters. An advantage of a theoretical study is that an ideal model can be established wherein a single parameter of the property of the material can be varied to observe how that parameter affects the characteristics of the material. In this study, the effect of surface structure and constituent atoms on the reactivity of surfaces are analyzed by comparing the dissociation of O_2 on clean (001) and (111) surfaces of Cu and Pt using first principle calculations within density functional theory (DFT). Here, the reaction pathway of O_2 dissociative adsorption on these surfaces is determined by calculation the total energy of the O_2-substrate system while varying the bond length r and center of mass distance Z of oxygen from the surface. As shown in Figure 1, the center of mass (c.m.) of oxygen is fixed at the bridge site of both surfaces (001) and (111) while both O atoms dissociate towards the hollow sites.

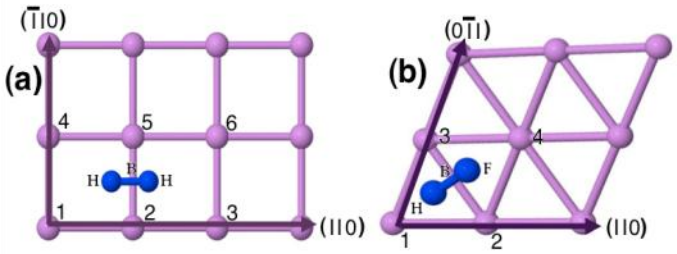

Figure 1. Top view of the model in calculation. (a) (001) surface, (b) (111) surface. The blue balls denote oxygen and the pink balls denote Cu (or Pt). "H", "B", "F" denote the hcp hollow site, bridge site, and fcc hollow site respectively.

In order to provide a physical description of the reactive pathway, the potential energy surfaces (PESs) and the density of states (DOS) relevant to the dissociative adsorption of O_2 on the (001) and (111) surfaces of Cu and Pt are presented.

2. Computational Model

Performing reliable calculation is important in order to get reasonable results. The parameters need to be determined carefully. Lattice parameters are determined by getting the energy minima of total energy of bulk system by varying the lattice parameter. The lattice constants are 3.64Å for Cu and 3.97Å for Pt, which are in agreement with experimental data 3.601Å[4] for Cu and 3.923Å[5] for Pt. Figure 2 and 3 show the total energy calculation of bulk of Cu and Pt respectively. The isolated O_2 molecule stable gas phase bond length is 1.23Å and dissociation energy is 6.02eV which has good agreement with experiment[6]. The cut-off energy for both systems (O_2 dissociative adsorption on Cu and O_2 dissociative adsorption on Pt) is 740 eV, which is determined based on convergence of total calculation for each component atom. Figure 4 shows the convergence of cut-off energy of the isolated O_2 molecule in stable gas phase by total energy calculation. The surface Brillouin zone integration is performed using the special-point sampling technique of Monkhorst-Pack k-point with 8x8x1 meshes. Figure 5 shows the convergence energy of k-points meshes for bulk Cu (one atom in one unit cell). Spin-polarized total energy calculations using Projector Augmented Wave (PAW) method [7,8] and plane-wave basis set are performed within DFT [3] framework by usingVienna *ab initio* simulation program (VASP)[9-12]. The generalized gradient approximation (GGA) of Pedrew, Burke, and Ernzerhof (PBE) is used for the exchange-correlation functional [13,14]. To model the situation with O_2 and metal surfaces, five layers of fcc(001) surfaces and four layer of fcc(111) surfaces for both Cu and Pt are used. The number of layers is varied until the local density of states (LDOS) of the atom in the middle of the layers resembles that of the atom in the bulk system. Layers are separated by 17Å vacuum which is large enough to avoid the surface interaction along z axis.

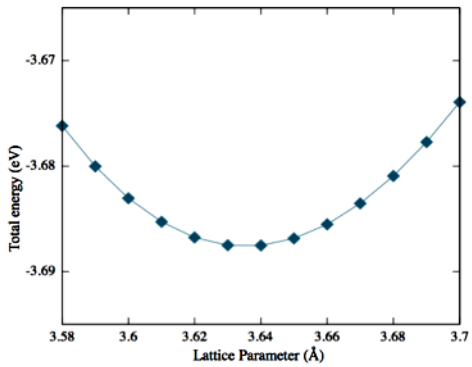

Figure 2. Total energy as a function of lattice parameter for Cu bulk.

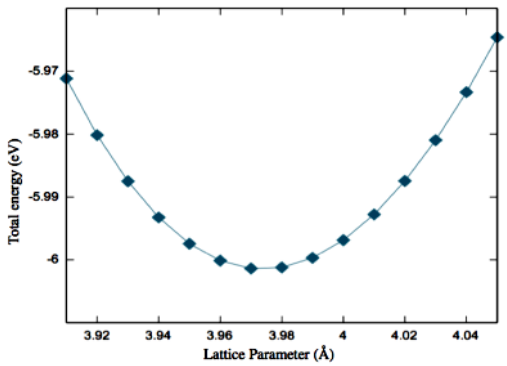

Figure 3. Total energy as a function of lattice parameter for Pt bulk.

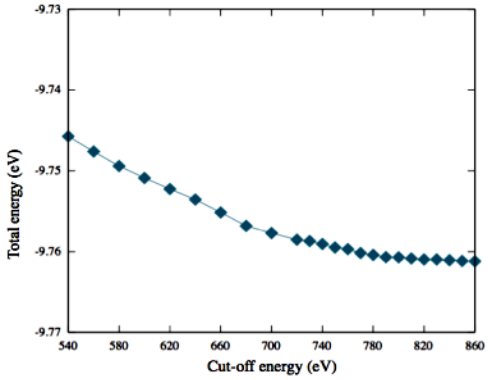

Figure 4. Total energy of isolated O_2 molecule as a function of cut-off energy, the accuracy here determined three digits of decimal. The energy converge around 740 eV.

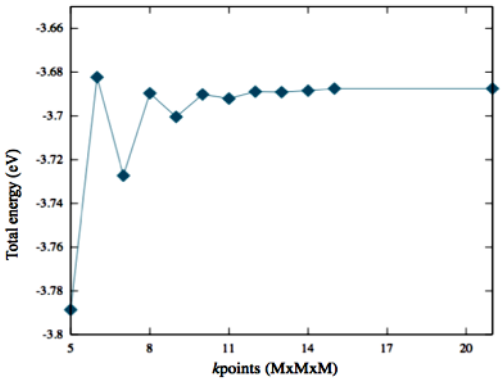

Figure 5. Total energy calculation of one atom Cu bulk as a function of k-points (MxMxM), the energy start to converge at k-points around 8.

As shown in Figure 1, the symmetric O_2 dissociative adsorption sites on (001) and (111) surfaces are considered in this study. The H-B-F site shown in Figure 1(b) on the (111) surface corresponds to the case when the c.m. of O_2 molecule is fixed at the bridge (B) site. After dissociation, O atoms are positioned at the hcp (H) and fcc (F) hollow sites. These configurations are chosen among all the possibilities since they allow the maximum (nearest) approach of the O_2 c.m. to the corresponding surfaces. The orientation of the O-O bond is kept parallel to the surface. Energies are given in eV relative to the values of the energy surface and isolated O_2.

3. Results and Discussion

The potential-energy surfaces for O_2 dissociative adsorption are shown on both the (111) and (001) surfaces of Cu in Figure 6 and Pt in Figure 7, as a function of O_2 bond length r and O_2 center of mass distance normal to the surface Z. The potential-energy surfaces of (111) and (001) surfaces are indicated (a) and (b) in both figures, respectively. The contour spacing is 0.1 eV in all figures. The dashed arrows indicate the reaction pathways for each case, and the corresponding values of activation barrier and adsorption energy are also indicated. The PESs for Cu and Pt surfaces show different characters. On Cu surfaces, O_2 undergoes two activation barriers for dissociative adsorption while for Pt surfaces O_2 only faces one activation barrier. If the reactivity of Cu and Pt is compared, O_2 easily dissociates on Cu rather than Pt whereas the activation barriers of Pt are bigger than the activation barriers of Cu.

The PESs corresponding to (001) and (111) surfaces of Cu and Pt are shown in Figure 6 and 7. Both activation barriers and adsorption energies on (001) surface are smaller than those on the (111) surface. This result is in good agreement with previous studies that the surface structure affects the reactivity which is conclude that the (001) surface is more reactive than the (111) surface [15,16]. Also, as indicated in both figures, O_2 can approach (001) surface closer than on (111) surface which makes the adsorption energy of O_2 higher on (001) rather than on (111) surface. And also this result of O_2 dissociation on Cu(001) is in good agreement with experimental studies of surface of measuring sticking coefficient of the incoming O_2 molecules [17,18]. The sticking coefficients have been found to be very low at small energies which imply that there is small dissociation barrier for the O_2 dissociation on clean Cu(001). This calculation has revealed this barrier which was not revealed by previously reported study[19].

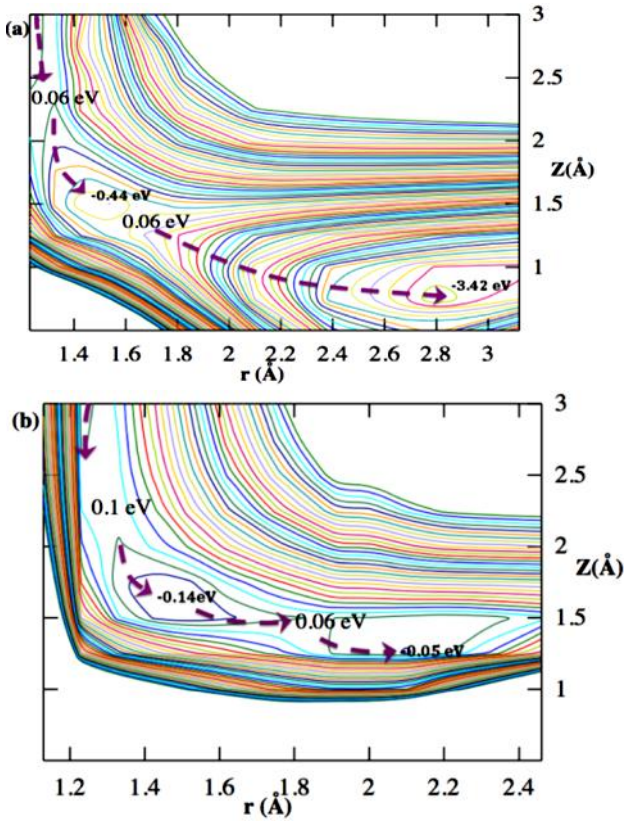

Figure 6. Contour plots of the potential-energy surfaces for O_2 dissociative adsorption on (a) Cu(001) and (b) Cu(111), as a functions of the O_2 bond length r and O_2 center of mass distance normal to the surface Z. The contour spacing is 0.1 eV. The dotted arrows indicate reaction pathways.In this figures, two activation barriers are indicated.On (a) Cu(111), the activation barriers are located (r,Z)~(1.23,2.25) and (r,Z)~(1.68,1.5) with the same value 0.06 eV. The adsorption sites located (r,Z)~(2.8,0.75) and (r,Z)~(1.43,1.5) with value -3.42 eV and 0.44 eV respectively. On (b) Cu(001), the activation barries are located (r,Z)~(1.23,2.25) and (r,Z)~(1.88,1.5) with value 0.1eV and -0.05eV respectively. The energies are given in eV relative to the value of isolated O_2 in stable gas phase and the surface.

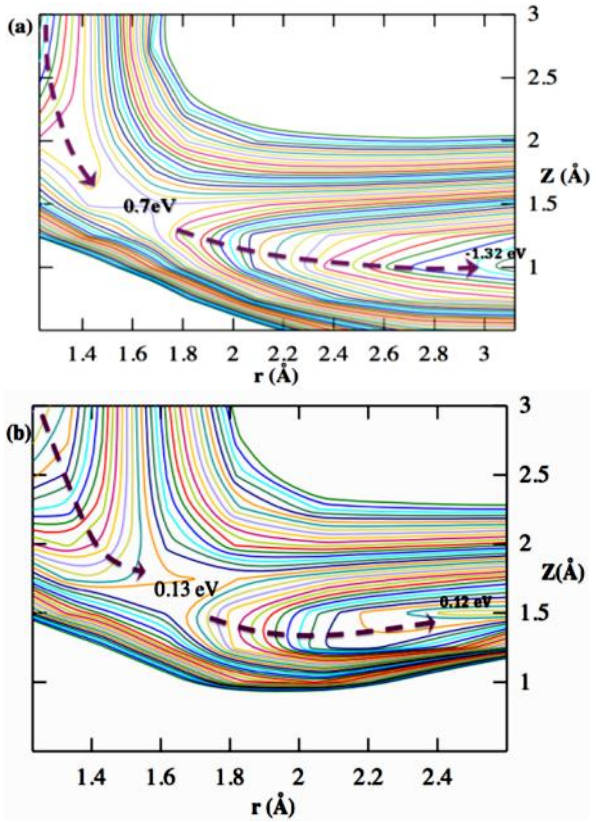

Figure 7. Contour plots of the potential-energy surfaces for O_2 dissociative adsorption on (a) Pt(001) and (b) Cu(111), as a functions of the O_2 bond length r and O_2 center of mass distance normal to surface Z. The contour spacing is 0.1 eV. The dotted arrows indiace reacton pathways. On (a) Pt(001), the activation barrier is located (r,Z)~(1.43,1.5) with a value 0.7eV, and the adsorption site located (r,Z)~(3.12,1) with a value -1.32eV.On (b) Pt(111), the activation barrier is located (r,Z)~(1.62,1.5) with a value 0.13eV, and the adsorption site located (r,Z)~(1.46,1.5) with a value 0.12 eV. The energies are given in eV relative to the value of isolated O_2 in stable gas phase and the surface.

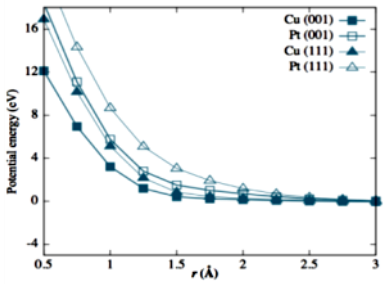

Figure 8. The corresponding energy plots when O_2 molecule approaches the Cu and Pt surfaces, with its bond length fixed at r=1.23Å. The difference starts to occur at Z~2.25Å, the results of Cu show lower energies rather than the results of Pt. There are no drastic changes in the trends.

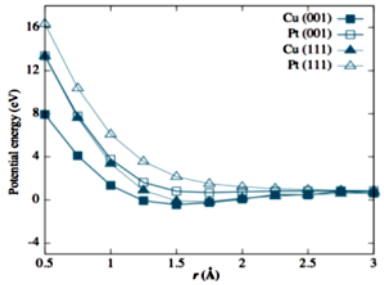

Figure 9. The corresponding energy plots when O_2 molecule approaches the Cu and Pt surfaces, with its bond length fixed at r=1.43Å. At 1.75Å ≤ Z ≤ 1.25Å, the results for Cu (001) and (111) surfaces show some changes in the trends. The trends of Pt are not change significantly from r=1.23Å.

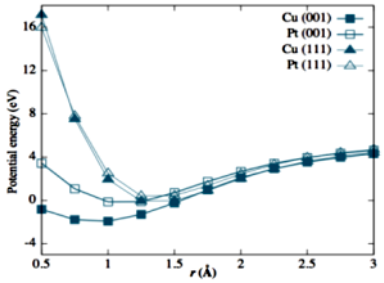

Figure 10. The corresponding energy plots when O_2 molecule approaches the Cu and Pt surfaces, with its bond length fixed at r=2.0Å. At Z≤ 1.75Å, the results for (001) and (111) surfaces show some differencefor both Cu and Pt. The results for (111) for both Cu and Pt are almost the same.

To clarify the origin of the difference in the corresponding PES in each case, some relations between Z and potential energies of the PESs are plotted at r=1.23Å, r=1.43Å, and r=2.0Å. This corresponds to the comparison of molecular adsorption, molecular precursor state adsorption, and quasiatomic adsorption respectively. Here, "quasiatomic" means that oxygen does not dissociate completely.

Figure 8 shows the corresponding energy plots when the O_2 molecule approaches the Cu and Pt surfaces with its bond length fixed at r=1.23Å. The four cases show the same trends. The energies begin to increase as O_2 molecule approaches the surface. However, when Z≤ 2.25Å the energies of Cu cases are lower compared to Pt cases. This indicates that O_2 molecule can approach Cu surface closer rather than Pt surface, in this sense such energy difference between Cu and Pt likely to be attributed to the hybridization strength between O_2 and metal surfaces since the radius atom of Cu smaller than the radius atom of Pt. Figure 9 shows the corresponding energy plots when the O_2 molecularly approaches the Cu and Pt surfaces with its bond length fixed at r=1.43Å. This bond length corresponds to consideration of O_2 adsorption as meta-stable process or molecular precursor state. In case of Cu, the trends start to differ from when r=1.43Å and at Z=1.5Å, potential energies are negative. On the other hand, for the case of Pt surfaces the trends are not really changed when at r=1.43Å. This indicates that dissociation via molecular precursor state tends to occur for the case of Cu surfaces. Figure 10 shows the corresponding energy plots when the O_2 approaches the Cu and Pt surfaces with a fixed bond length r=2.0Å. The four cases almost show the same energies from Z=3.0Å and drastically change when Z≤ 1.5Å. The plots begin to differ depending on surface structure. The oxygen atoms on (001) surface can avoid energy increment compared with that on (111) surface where the oxygen atoms tend to expand to bond length of over 2Å. Considering the local structure of the surface as shown in Figure 1, when the oxygen approaches the (111) surface, as it expands to bond length r=2.0Å or larger. Repulsion between oxygen atoms at "1" or "4" site of Figure 1(b) increases the potential energy, while (001) surface has no metal atoms near the expanding oxygen in the first layer. The differences of the PESs are more apparent in the case of r=1.43Å and r=2.0Å rather than that of r=1.23Å. In other words, the difference between the case of Cu and Pt is mainly attributed to the appearance of molecular precursor state in that case of Cu. On the other hand, quasiatomic adsorption

mainly attributes to the difference in surface structure. The adsorption energy on (001) surface is further reduced with increasing *r* up to around ~3Å.

These results are in good agreement with a series of experiments showing the oscillating behavior in oxidation of CO on Pt surface, which also shows that the reactivity of oxygen has improved by changing surface structure from hexagonal to the (001) surface [20-22]. Based on the results, of O_2 dissociative adsorption on Cu surfaces are mediated by molecular precursor state. In the case of O_2 dissociative adsorption on Cu(111) at the precursor state (r,Z)~(1.43,1.5), the system is magnetized with unit magnetic moment of ~1μB. This magnetization comes from the oxygen which indicates that superoxo-like (O_2^-) occurs then O_2 subsequently dissociates to quasiatomic state. This result has a good agreement with experimental results [23,24] wherein the chemisorption molecular precursor state was found in O_2 dissociative adsorption on Cu (111). On the other hand, O_2 dissociation on Cu (001) is also found as molecular mediated precursor at the precursor state (r,Z)~(1.43,1.50) then transfer electron to O_2 molecule ~1 electron. It indicates that molecular precursor mediated by superoxo-like (O_2^-) occurs, however, this result of O_2 dissociative adsorption on clean Cu(001) surface has discrepancy with STM experimental [25] result wherein direct dissociation is likely to happen. This discrepancy may be explained by the static calculation used in this study.

4. Conclusion

In summary, DFT-based total energy calculations have been invoked in order to investigate the difference in the dissociative adsorption of O_2 on two types of Cu and Pt surfaces, viz., Cu(001), Cu(111), Pt(001), and Pt(111). Of the several parameters that might govern to reactivity of O_2 dissociative adsorption, the focus here is the static effect of surface structure and constituent atoms. The reactive pathways are derived from the trace of energy minimum under the same conditions. Results show that the difference in O_2 dissociative adsorption on the different surface structures is given by the quasiatomic adsorption on (111) and dissociative adsorption on (001) surface. The quasiatomic adsorption on (111) surface is due to the local structure of the surface. Also, changing the surface structure affects the surface reactivity of O_2 dissociative adsorption. Here, (001) surface is more reactive than (111) surface because of the lower activation barrier and higher adsorption energy at the former than the latter. The difference in O_2 dissociative adsorption for different constituent atoms is given mainly by adsorption which is mediated by precursor states on Cu and direct dissociation on Pt.

References

1. IE. Maxwell, Science 101, 1 (1996).
2. M. Okada, K. Moritani, A. Yoshigue, Y. Teraoka, H. Nakanishi, W. A. Dino, H. Kasai, T. Kasai, Science 301, 315 (2004).
3. P. Hoenberg and W. Kohn, Phys. Rev. B, 136, 864 (1964).
4. Takaya Fujita, Yuki Okawa, Yuji Matsumoto, and Ken-ichi Tanaka, Phys. Rev. B. 54, 2167 (1996).
5. G. W. R. Leibbrandt, R. van Wijk, and F. H. P. M. Habrake, Phys. Rev. B. 47, 6630 (1992).
6. CRC Handbook of Chemistry and Physics, 86th ed., CRC Press, Boca Raton, FL, (2005).
7. P.E. Blöchl, Phys. Rev. B, 50, 17953 (1994).
8. G. Kresse, J. Joubert, Phys. Rev. B, 59, 1758 (1999).
9. G. Kresse, J. Furthmüller, Comput. Mater. Sci. 6, 15(1996) .
10. G. Kresse, J. Furthmüller, Phys. Rev. B, 54, 11169 (1996).
11. G. Kresse, J. Hafner, Phys. Rev. B, 47, 558 (1993).
12. G. Kresse, J. Hafner, Phys. Rev. B, 49, 14251 (1994) .
13. J.P. Perdew, K. Burke, M. Ernzerhof, Phys. Rev. Lett. 77, 3865 (1996).
14. J.P. Perdew, K. Burke, M. Ernzerhof, Phys. Rev. Lett. 78, 1396 (1997) .
15. S. Yotsuhashi, Y. Yamada, W. A. Diño, H. Nakanishi, and H.Kasai, Phys. Rev. B 72, 033415 (2005).
16. M. Okada, K. Moritani, A. Yoshigoe, Y. Teraoka, H. Nakanishi, W. A. Diño, H. Kasaiand T. Kasai, Phys. Rev. B, 77, 115413 (2008).
17. M. Okada, K. Moritani, S. Goto, T. Kasai, A. Yoshigoe, and Y. Teraoka, J. Chem. Phys. 119, 6994 (2003).
18. M. Okada, K. Moritani, A. Yoshigoe, Y. Teraoka. H.Nakanishi, W. A. Diño, H. Kasai, and T. Kasai, Science, 301, 315 (2004).
19. M. Alatalo, S. Jaatien, P. Salo, K. Laasonen, Phys. Rev. B, 70, 245417 (2004).

20. M. Eistwirth, P. Moller, k. Wetzl, R. Imbihl, Phys. J. Chem. Phys. 90, 510 (1989).
21. M. P. Cox, G. Ertl, and R. Imbihl, Phys. Rev. Lett. 54, 1725 (1985).
22. H. H Rotermund, W. Engel, M. E. Kordesch, and G. Ertl, Nature (London) 343, 355 (1990).
23. Spitzer, A.; Lu¨th, H. Surf. Sci.,118, 136 (1982).
24. Prabhakaran, K.; Sen, P.; Rao, C. N. R. Surf. Sci., 177, L971 (1986).
25. K. Yagyu, X. Liu, Y. Yoshimoto, K. Nakatsujiand F. Komori, J. Phys. Chem.C, 113, 5541 (2009).

Life as a Short Term Student in Osaka University

If there is one word to describe my life as a short term student here, it's no less than 'perfect!'.

As a short term student, I had a big chance to live in Japan, to know the Japanese culture, to deal with people here, to adapt with the University systems, and most of all, to become researcher. I have learned a lot of important new things that somehow changed the way I think before. I have been so blessed having the chance to experience how to become a researcher. Being a researcher is my dream since I was a high school student. I was enjoying science then, especially physics and mathematics, but when I have found that some researchers in my country seem not to really enjoy their job, especially their salary, I was a bit disappointed. That was one of reasons why I decided to enter engineering major rather than science.

At first it was so difficult for me to turn to another life immediately, especially my first experience to live separate from my family. Moreover, it's overseas. The first time I came here, there is no one I have ever known before. All things around me are new: new people, new weather, new culture, new rules, new language, and new life. As we know, to go to the next higher state, we must face a transition state which is always troublesome. Turning to become "doing everything by my elf only" was quite difficult for me. I need to manage my money, cook, pay insurance, pay rent room, clean room and do grocery. But now I have learned to do those things. I started get used to those things. I am now living as an adult person.

The most difficult thing I have done here is training myself to become a good researcher. I tried to watch, listen, understand and try to do what others do. Most of the things being done in the laboratory are entirely different from where I am used to. Not only working hard is required here, but also the good attitude as a researcher. I should learn to appreciate researches of my labmates, be criticized, give input to each other, realize opportunity, care for details and clearness, deal with people who have different opinions, cooperate, encourage each other, become honest either to our self or the other, become brave to tell our thoughts, resolve my confusion, struggle on what we thought is right, ask for discussion and not to get answered, and the most is to know that what I am doing is something which nobody else knows. These made me thing that it is necessary to keep studying to enrich my knowledge to be able to answer the unanswered problems. As a student, I always get answers from the book. I get achievements by doing some structural steps. I learn other thought to get my problem answered. I always get someone point me out the steps to get achievement or to get the answer. I ask the lecturer to get the answer. I study hard to pass the test. I study harder to get higher score and to compete with other students. Those are all entirely different when I entered this research community. Frankly, all of those gave me incredibly stress. Many times I get lost and don't know what to do. Many times I failed. Many times I tried to escape from the problems. And many times I tried to give up. But amazingly, those new people around me helped me and rised me up. I always get someone to encourage me. I always get someone help me. I always get someone to care for me. I always get someone to ask if something is wrong with me. I always get someone help me if I am in trouble. I always get someone cheer me up. I always get someone say "you can do it!". All of those always bring myself back to "*ganbatte*" many times. All of those are the best things that I got

here! I feel so happy to be here, in Kasai-lab, which has incredible members. It doesn't matter if they are Japanese students, Indonesian students, other foreigner students, staffs, senpais or supervisors. All of them just do not mind to help me. Honestly, it is only here where I got different relationship between students and staff. The staffs here are so friendly. We really had a good relationship and we respect each other. I have learned a lot from all of them. I really owe them a lot. I feel like having a family here. We laugh together, we share things, we make memories, or we even fight. They just make me feel that I belong to the community as well. All of those helped me in my struggle during the hard "transition" time. That is really a big awesome thing for me as an overseas student. *Hontou ni doumo arigatou gozaimasu*!.




I am really grateful to the QED short term program, to Kasai-sensei and to Hermawan-sensei who supported me here. I got enough scholarship to support my life here in Japan so tha I can focus on my research. For that, I am really grateful to JASSO. I got an adorable sensei here. He is so humble but so great and knows a lot of things as well. I get awesome friends and family here. All of these made my life perfect here in Japan. I will keep on learning. I will do the best that I can. I do not want to disappoint anyone who has worked hard and shared their time to teach and help me here in Japan. I really owe many things to everyone here. Thank you very much from the deepest part of my heart.

With love,
Cica Gustiani
Indonesia

Synthesis of Novel Ligand Molecules Based on Tetrakis(2-pyridyl)methane

Elisha Gabrielle Verzosa Tiu

Department of Chemistry, Graduate School of Science, Osaka University, Japan

Abstract

Tetrapyridylmethanes are one of the most important members of tetrakis(heteroaryl)methanes. In this study, tetrakis(2-pyridyl)methane has been synthesized in excellent yield. Two possible synthetic methods are examined and it has been found that the nucleophilic aromatic substitution with 2-fluoropyridine is the effective one. ^{1}H and ^{13}C NMR analyses confirm the structure of the synthesized molecule which is indeed the highly symmetrical tetrakis(2-pyridyl)methane.

1. Introduction

In 1897, Gomberg successfully synthesized tetraphenylmethane[1]. Since then tetraphenylmethane and its properties have been extensively studied. However, tetrakis(heteroaryl)methanes, a close similar in structure with tetraphenylmethanes, only bearing heteroaromatic rings instead of phenyl rings, have never been studied. This may be due to the difficulty in the synthesis of these compounds. Tetrakis(heteroaryl)methanes have very interesting properties. The positional isomers that may be constructed, for one, is quite unique from tetraphenylmethane. Tetrakis(heteroaryl)methanes are even more interesting in terms of their structure and functionality. Indeed, research on tetrakis(heteroaryl)methanes is very promising in many aspects.

It is well known that tetraphenylmethanes are synthesized by electrophilic aromatic substitution, since benzene rings are known for its reactivity to this reaction. However, such is not always the case for tetrakis(heteroaryl)methanes. It is not favorable for pyridine to go through electrophilic aromatic substitution reaction. Also, since tetrapyridylmethyl cations would be electronically unstable, such entities have never been identified. Due to these reasons, tetrapyridylmethanes were thought to be very difficult to synthesize.

Pyridine is one of the most popular heteroaromatics that are known. It is well known that the sp^2 hybridized nitrogen of pyridine (Figure 1) has basicity and coordination ability. Connecting 4 pyridine rings together with a sp^3 hybridized carbon atom yields tetrapyridylmethanes. Interestingly, these have 15 positional

isomers, and among them tetrakis(2-pyridyl)methane, tetrakis(3-pyridyl)methane, and tetrakis(4-pyridyl)methane are the most appealing ones, since they have the higher symmetry.

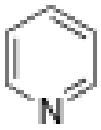

Figure 1. Pyridine.

Tetrapyridylmethanes can be novel ligand molecules. Metal complexes of tetrapyridylmethanes may have various interesting properties, for example, spin crossover behavior. In this study, tetrakis(2-pyridyl)methane (**1**) has been successfully synthesized in excellent yield.

Tetrakis(2-pyridyl)methane (**1**) is chosen to be synthesized first among these isomers, because nucleophilic aromatic substitution will lead to the tetrakis(2-pyridyl) and tetrakis(4-pyridyl), *ortho* and *para* positions, respectively. On the contrary, it is expected that obtaining tetrakis(3-pyridyl) or the *meta* position is even more challenging.

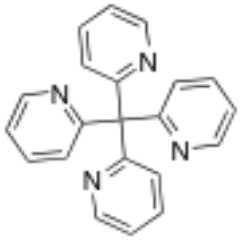

Figure 2. Tetrakis(2-pyridyl)methane (**1**).

Tetrakis(2-pyridyl)methane can form metal complexes with the various transition metals. It is a chelating ligand whose metal complexes can have properties of a molecular magnet, catalyst, and spin crossover behavior. Spin crossover phenomenon is very interesting because there can be many possible applications. The objective of this study is to be able to successfully synthesize tetrakis(2-pyridyl)methane and the related ligand molecules.

2. Experimental section

In order to synthesize the target molecule tetrakis(2-pyridyl)methane, there are two possible synthetic routes that may be used. Gomberg and Kamm in 1917 studied about the synthesis of tetraphenylmethanes [2]. They synthesized tetraphenylmethane by reacting triphenylchloromethane and phenylmagnesium bromide in

high temperatures and ether-free solvent environment. However, the yield was low, about 10 to 12% yield. Another study by Schoepfle and Trepp, stated that they obtained tetraphenylmethane in 5 to 6% yield and biphenyldiphenylmethane in 65 to 76% yield [3]. Although tetraphenylmethane was retrieved in low yield, it was retrieved nonetheless. This gives us an insight that the similar method may be applicable to the tetrakis(2-pyridyl)methane. The second route that may be possible for the synthesis of tetrakis(2-pyridyl)methane is the nucleophilic aromatic substitution of 2-halopyridines with tris(2-pyridyl)methyl anion. The halogens in the 2-halopyridines were varied by changing it from Br to Cl to F. Since Cl and F are both more electronegative than Br, it can be inferred that 2-chloropyridine or 2-fluoropyridine may be more reactive than 2-bromopyridine. It is well-known that the 2- and 4-halopyridines are susceptible to nucleophilic aromatic substitution. The reaction of tris(2-pyridyl)methyl anion and 2-halopyridines may also be an efficient route towards the synthesis of tetrakis(2-pyridyl)methane.

2.1 Route A

In order to synthesize the target compound tetrakis(2-pyridyl)methane, tris(2-pyridyl)chloromethane (**2**) was reacted with 2-pyridyllithium. 2-Pyridyllithium was formed by lithiating 2-bromopyridine with 0.9 equivalents of *n*-butyllithium at −70 ^{o}C. To a solution of 2-pyridyllithium was added 1.0 equivalent of compound **2** (Scheme 1). It is expected that tetrakis(2-pyridyl)methane might be formed by the replacement of the Cl in compound **2** with the pyridine in 2-pyridyllithium. However, the target compound was not obtained at all.

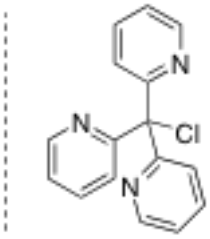

2

Scheme 1. Route A to tetrakis(2-pyridyl)methane.

2.2 Route B

A 300 mL 4-necked flask was equipped with 2 stoppers, septum, dropping funnel, and reflux condenser and N_2 balloon. The set up was dried under vacuum by heat gun. The set-up was filled with nitrogen gas.

A solution of tris(2-pyridyl)methane (450 mg, 1.8 mmol) in mesitylene (20 ml) was charged in the flask. The set up was cooled up to 0 ^{o}C and was added with 2.0 mmol of *n*-butyllithium in hexane in a dropwise fashion under nitrogen atmosphere. The solution was stirred for 1 hour at 0^{o}C. The resulting reddish orange solution was added to 0.77 ml or 9.0 mmol 2-fluoropyridine. The temperature was slowly increased to room temperature and then was refluxed for 24 hours. After cooling it again to 0 ^{o}C, distilled water was added. The mixture was then extracted with ethyl acetate and chloroform repeatedly. The combined organic layers were dried over anhydrous Na_2SO_4. The solvent was evaporated and the remaining residue was purified even more by column chromatography on alumina eluted with ethyl acetate. Recrystallization was done to retrieve a pure crystal form. The solvent for recrystallization was ethyl acetate –chloroform (3:1 v/v). Tetrakis(2-pyridyl)methane (**1**) was finally retrieved in 543 mg, 93% yield. The appearance of **1** was colorless, needle-like crystals.

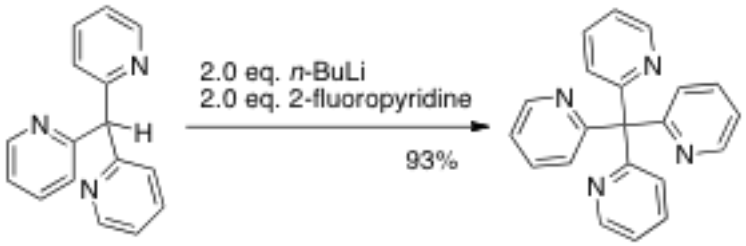

Scheme 2. Route B to tetrakis(2-pyridyl)methane. The target compound was successfully obtained in excellent yield.

3. Results and Discussion

3.1 Route A

Route A (Scheme 1) did not give the desired results for tetrakis(2-pyridyl)methane. The reaction only yielded carbinol compound **3** in 36% yield, and tris(2-pyridyl)chloromethane **2** was recovered in 39% yield. Since the central carbon in compound **2** is sterically hindered, the reaction did not occur. A halogen-lithium exchange between 2-pyridyllithium and **2** followed by the oxidation with oxygen, took place instead, thus explaining the formation of compound **3**. Since 2-pyridyllithium is unstable at higher temperatures, the reaction could not be carried out at higher temperatures. Since Route A failed, the use of 2-halopyridines as reagents was implemented, Route B.

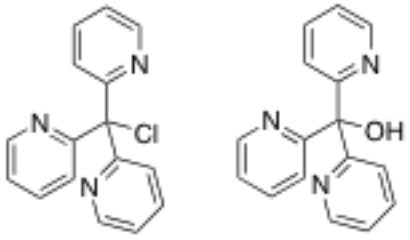

2 **3**

Figure 3. Compound **2** and compound **3**, obtained products for route A.

3.2 Route B

For the nucleophilic aromatic substitution of 2-halopyridine with tris(2-pyridyl)methyl anion, three kinds of 2-halopyridines were used, 2-bromopyridine, 2-chloropyridine and 2-fluoropyridine.

3.2.1 2-Bromopyridine

The target compound tetrakis(2-pyridyl)methane was not retrieved by using 2-bromopyridine as a reagent. Refluxing a mixture of tris(2-pyridyl)methyl anion and 5.0 equivalents of 2-bromopyridine for 48 h, only yielded a dimeric substance **5**. This result may be attributed to the formation of tris(2-pyridyl)methyl radical **4** as intermediate. A single electron transfer has occurred on tris(2-pyridyl)methyl anion to 2-bromopyridine, thus forming the radical **4**. The radical **4** was dimerized and a 1,5 proton transfer of the dimer gave the product **5**.

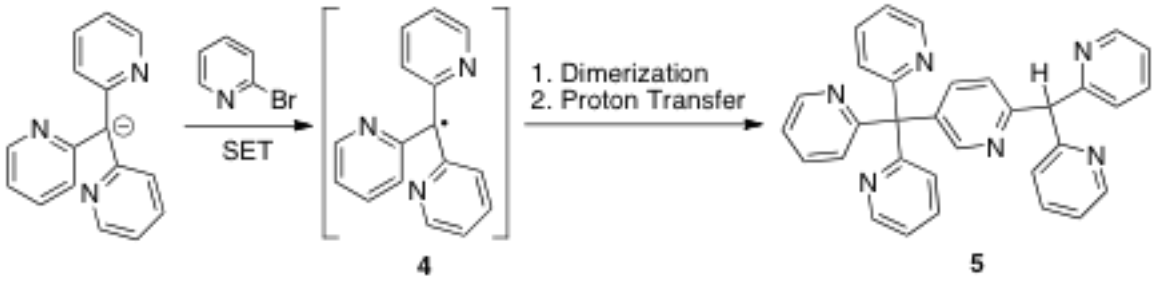

4 5

Scheme 3. Reaction of tris(2-pyridyl)methyl anion with 2-bromopyridine to form **5**.

3.2.2 2-Chloropyridine and 2-fluoropyridine

Since the reaction did not yield the target compound tetrakis(2-pyridyl)methane when 2-bromopyrdine was used, maybe due to the low reactivity of 2-bromopyridine and the steric hindrance around the central carbon atom in tris(2-pyridyl)methyl anion, the similar reactions were carried out with 2-chloro and 2-fluoropyridine.

By using 5.0 equivalents of 2-chloropyridine as one of the reagents in THF, the target molecule was obtained; only it was in a low yield of 1%. By changing the solvent to mesitylene, the yield was increased to

52% (Table 1). On the other hand, by using 5.0 equivalents of 2-fluoropyridine in mesitylene and then refluxing for 24 hours, the target compound was retrieved in a high yield of 93%.

Table 1. Solvents used and respective percentage yield of tetrakis(2-pyridyl)methane (**1**).

Entry	Solvent	X	Yield /%		
			$(2\text{-Py})_4\text{C}$ (**1**)	$(2\text{-Py})_3\text{CH}$	$(2\text{-Py})_3\text{COH}$ (**3**)
1	THF	Cl	1	80	0
2	Toluene	Cl	6	89	4
3	Xylene	Cl	28	65	6
4	Mesitylene	Cl	52	47	0
5	Mesitylene	F	93	4	0

3.3 Properties of tetrakis(2-pyridyl)methane

The target molecule tetrakis(2-pyridyl)methane is a colorless crystal, with melting point at 259–260 °C. It is soluble in $CHCl_3$ and $CHCl_2$, less soluble in benzene, CH_3OH, CH_3CN, and DMSO.

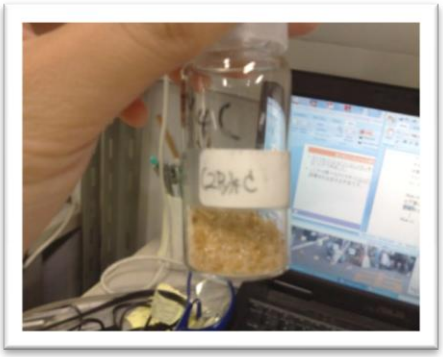

Figure 4. Tetrakis(2-pyridyl)methane.

3.4 NMR Spectrum

In the ^1H NMR spectrum shown in Figure 6 below, only the protons of one set of pyridine ring in tetrakis(2-pyridyl)methane is represented. Since the environment of the protons in each of the four rings are

the same, the peak in the NMR spectrum shows only the protons in one ring. The sample was run using a 400 MHz ^{1}H NMR, the sample in $CDCl_3$.

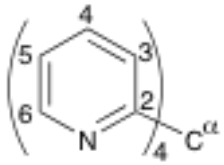

Figure 5. Pyridine rings of tetrakis(2-pyridyl)methane (**1**) with the same environment.

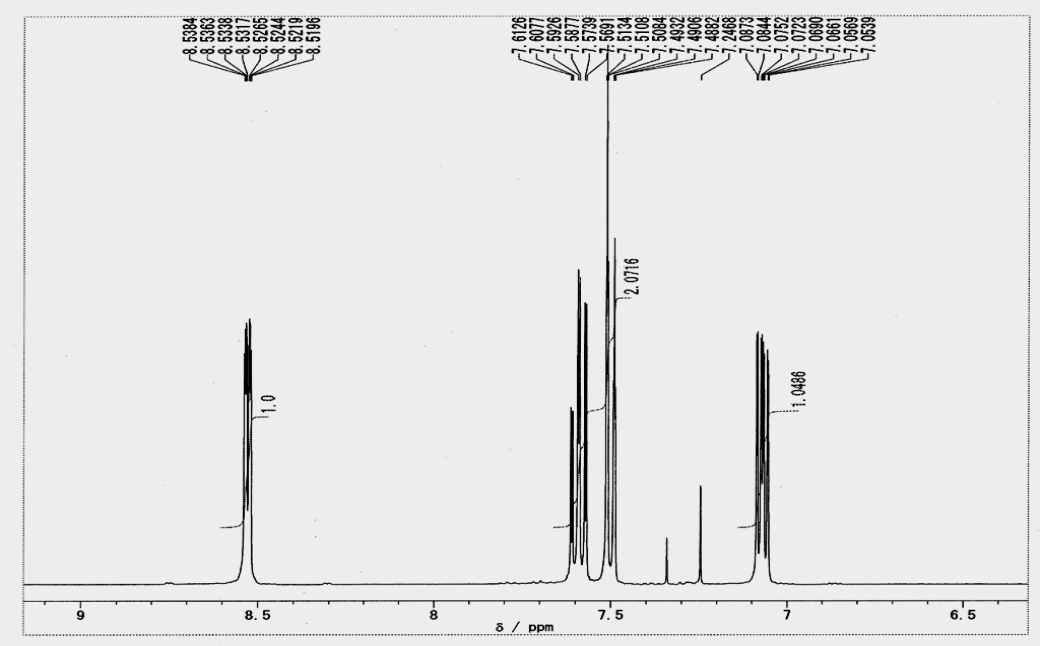

Figure 6. ^{1}H NMR chemical shifts of tetrakis(2-pyridyl)methane in $CDCl_3$.

Table 2. ^{1}H NMR data of tetrakis(2-pyridyl)methane.

H-6	8.53	ddd	5.0, 1.9, 1.0	4H
H-5	7.07	ddd	7.7, 5.0, 1.0	4H
H-4	7.59	td	7.7, 1.9	4H
H-3	7.50	dt	7.7, 1.0	4H

The coupling constants that may be retrieved from the ^{1}H NMR spectrum shown in Figure 6 may help in determining which proton is represented by which signal. Experimental data of the coupling constants *J* were compared with the typical values for the chemical shifts and coupling constants of pyridine. [4]

^{13}C NMR was also performed for the confirmation of the structure of the synthesized compound. It was conducted at 100 MHz, the sample in $CDCl_3$. Chemical shifts are shown in tabulated form (Table 3).

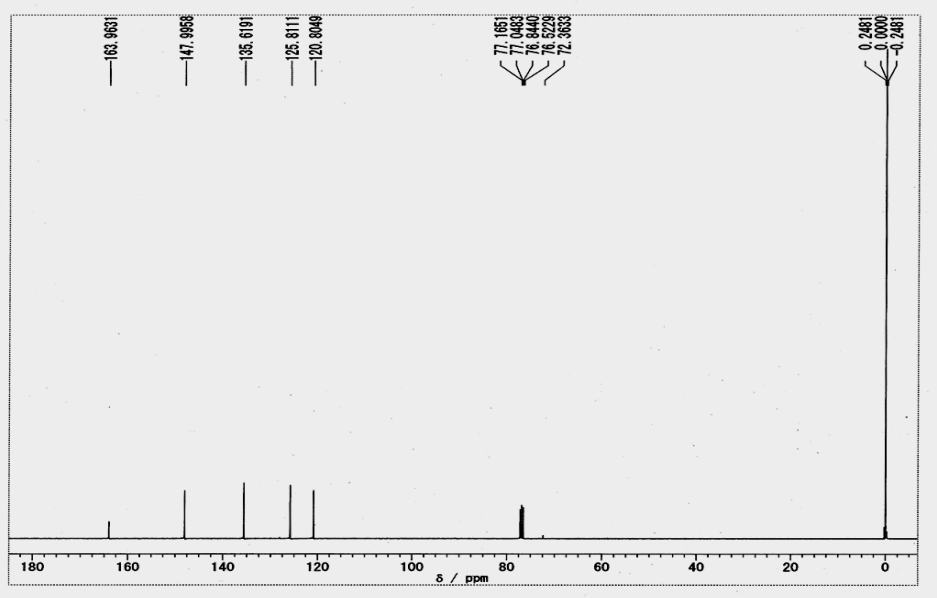

Figure 7 ^{13}C NMR chemical shifts of tetrakis(2-pyridyl)methane in $CDCl_3$.

Table 3. Experimental chemical shifts of carbon atoms in ^{13}C NMR.

Assignment	Chemical shift, δ / ppm
C-α	72.36
C-2	163.96
C-3	125.81
C-4	135.62
C-5	120.80
C-6	148.00

The experimental values of ^{13}C NMR spectrum is shown in Figure 7 match the literature values of ^{13}C NMR spectrum of pyridine. These values further confirm that the synthesized molecule was indeed tetrakis(2-pyridyl)methane.

4. Summary and Conclusion

In conclusion, tetrakis(2-pyridyl)methane has been successfully synthesized, which is clearly confirmed by its ^{1}H and ^{13}C NMR spectra. Tetrakis(2-pyridyl)methane was obtained by the nucleophilic aromatic substitution of tris(2-pyridyl)methyl anion with 2-chloropyridine or 2-fluoropyridine, in 52% or 93% yield, respectively. Tetrakis(2-pyridyl)methane is a colorless, crystalline substance with melting point up to

259–260 ^{o}C. This crystal is soluble in $CHCl_3$ and CH_2Cl_2. Tetrakis(2-pyridyl)methane may be used as ligand molecule to form metal complexes which may have interesting properties such as spin crossover behavior.

Reference

[1] Silverstein, R.; Bassler, G.; Morrill T. Spectrometric Identification of Organic Compounds 5th ed.; John Wiley & Sons, Inc.:1963.

My Life as a QEDC Short Term Student

Approximately two years prior to the news that I was granted a scholarship to study in Japan, honestly, I have been praying and hoping of studying here. Learning and experiencing the life of a foreign student in Japan has been my long time dream. I would be lying if I said that there were no difficult or unpleasant times during the whole year. But just thinking about now- how my dream is becoming a reality before my eyes- is more than enough to keep me satisfied, happy, and cheerful throughout all the challenging moments, everyday. No words can describe perfectly the gratefulness I have in my heart.

I vividly recall how nervous I was on the day before I met all laboratory staff and members. I thought a lot about how my supervisor will be like, what the surroundings will be, how laboratory members will think about me, and all the things a foreign student ought to be worried about. *Maa, shoganai.* I was alone from now on; very unusual from my background, entirely unique from where I came from. All I was sure about was that, I was so fortunate to be here and that I will do my best.

As the months have passed, Kubo laboratory has grown to become very dear to me. Although it was clear to all that I was the only foreigner in the laboratory, it never occurred to me that I was a *gaikokujin.* In all honestly, I feel "homey" whenever I am with my laboratory mates. At least to me, they have become a second family. I have met a lot of great people from this laboratory. I guess I can say that, for me, staying in this lab was the best part of being a foreign student. Being in the laboratory made me want to work harder and speak Nihongo fluently, *Osaka-ben* too. I am especially thankful to the very *genki* Kubo-*sensei* and very *gaman duyoi* Matsumoto-*sensei*, who are two of the kindest, most *sugoi*, and most fatherly-like *senseis* whom I have met and probably will ever meet in my entire life. Whenever my friends meet my *senseis*, the next sentence they usually utter is that "your sensei is very *yasashii".* I know that only so well. They are always there to help me with just about anything. I am also especially thankful to Inokuchi-senpai. *Yappari*, whenever he is there, I always feel that I have a big brother in laboratory. He is one of the best people I have met in my life. I never recall a moment when he was tired of learning and teaching. I want to become a great scientist like my *senpai*.

In a year of my stay in Japan, I have learned not only about research, chemistry, and laboratory skills, but also about Nihongo and a whole lot about Japanese culture. I have met a lot of great people and gained a lot of good friends, not to mention all the pleasant memories which came along with them. This year-long journey has opened my eyes to the things which have seemed invisible to me before. It has led to a lot of doors and opportunities. It has pushed me to do my best and dream more. I will never forget this gift and in my heart, I want to return the favor. I pray that Japan will continue to be a channel of blessing to all the countries of the world, especially in education, as it is and will continue to be abundant in resources.

I will work harder and keep on being grateful every day. It may seem to most that this opportunity has already ended; however, to me, it has only just begun.

Tiu, Elisha Gabrielle Verzosa
Osaka, August 1, 2011

First principle study on hydrogen doped graphene

Gagus Ketut Sunnardianto

Abstract

Graphene has been predicted to possess many applications because of its unique properties. Pure graphene has no band gap and changing its electronic band structure is an interesting field of research. This study reports a method of controlling the band gap of graphene by hydrogen atom impurity. Density functional theory based calculations are performed to obtain the electronic band structure of grapheme with atomic hydrogen impurity. It is found that hydrogen impurity can cause the Fermi level of graphene to shift. 5% hydrogen coverage on top of graphene makes graphene become half-metal ferromagnetic. This property is very useful in the field of spintronics.

1. Introduction

Graphene as the mother building block of many carbon-based materials, has been predicted to possess many applications because of its unique properties. Graphene can be considered as a single layer of graphite in a structured hexagonal system. Several interesting applications of graphene have been revealed recently. One of the surprising phenomena on graphene is the change of its electronic band structure of depending on the impurities absorbed. The adsorption of atomic hydrogen on graphene is predicted to open the band gap. In this year, many groups reported the same work. They tried to make graphene as semiconducting material by using several adsorbates. In general, they used the similar method that is plane wave DFT and succeeded in creating electronic band gap in graphene. Based on these, the band gap of graphene could be controlled by selecting certain atoms or molecules that will be absorbed. This aspect brings graphene as a promising candidate for electronic device application in the future. In this study, the change of electronic band structure of graphene has been investigated by hydrogen atom impurity. All my calculations in this study have been performed using first principles electronic structure calculation based on density functional theory (code machikaneyama2002)

2. Theoretical Background

The Density Functional Theory is adopted as a tool for the calculation of the electronic structure. The main goal of any first principles computational method is to give the chemical composition and the geometrical structure of a system and to calculate its properties as precisely as possible by solving the electronic Schrödinger equation. These methods do not make use of any

empirical information. However, the problem of solving the Schrödinger equation to find the quantum ground state description of the electron in a solid system is correlated to many-electron problems, which can be solved only approximately. Density Functional Theory is now one of the most widely used methods to solve many electron-problems. It is an exact theory for interacting electrons, but in practice, it is an approximate methodology in terms of single electrons

P. Hohenberg and W. Kohn formulated the basis of this theory in 1964. They established that any property of a system of many interacting particles, in a external potential $\mathrm{V}_{\mathrm{ext}}(r)$, can be seen as a functional of the density of particles in its ground state $\mathrm{n}_0(r)$. In this way, given the functional of $n_0(r)$. It is possible to get all the information of the systems.

The Density Functional Theory is based on only two theorems :

1. For any system of interacting particles in an external potentials $\mathrm{V}_{\mathrm{ext}}(r)$, the potential $V_{ext}(r)$ is determined uniquely by the ground density $n_0(r)$.
2. For any particular $V_{ext}(r)$, the exact ground state energy of the system is the global minimum values of the energy functional $\mathrm{E}[\mathrm{n}]$, and the density $n_0(r)$ that minimize the functional is the exact ground state density $n_0(r)$.

These can be expressed in other words: the density of particles in the ground states uniquely determines the external potentials $\mathrm{V}_{\mathrm{ext}}(r)$ acting on them and vice-versa. Therefore, all the properties of the system, including the ground state wave function ψ_0 and all derived observable are uniquely determined by $n_0(r)$

3. Computational Model

Before investigating the interaction between H and graphene plane, the geometrical structure of graphene has to be optimized. Atomic H does not need any optimization process since it only exists as single atom. The bond length of C-C and lattice parameter of graphene are found by varying the distance between two carbon atoms in hexagonal configuration. The exact bond length is the most stable position. It will be achieved when the total energy reaches the most negative value.

The binding energy between H and graphene can be achieved by employing :

$$\mathrm{E}_{\mathrm{bind}} = E_{C-X} - E_C - E_X$$

Here, $E_{C\text{-}X}$ represents the total energy of the graphene-X system (X refers to H), E_x is the energy of isolated X atom and E_C is the total energy of graphene. The exact bond length has been achieved when the binding energy reaches the most negative value

The graphene structure used in hydrogen adsorption study is an infinite graphene sheet. Hydrogen atom was randomly placed at the top site.

Before calculating the density of states of graphene due to impurity, I calculated the density of states of pure graphene first. For this purpose, I only used a simple structure consisting of two carbon atoms. To calculate the density of states of impure graphene, I used an infinite graphene sheet and hydrogen atom as impurities located randomly on top of carbon atom.

4. Results and Discussion

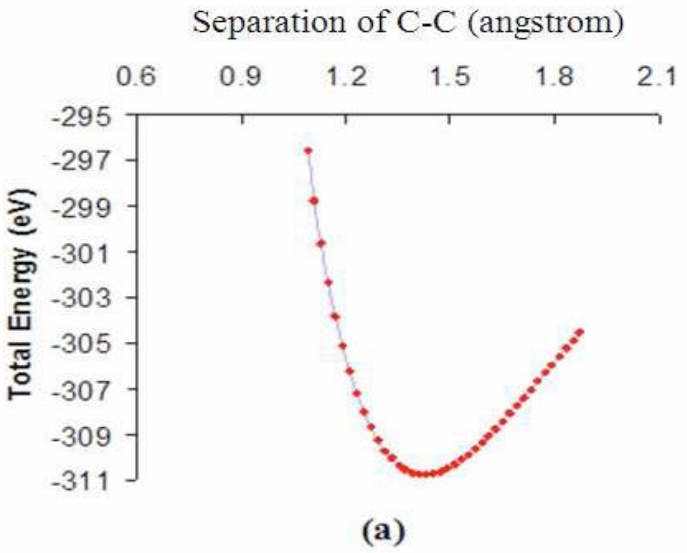

Figure 1: The curve of total energy as a function of separation distance between two atoms (carbon-carbon bond in graphene)

The graph in Figure 1 shows the curve of total energy as a function of separation distance between carbon-carbon bond in graphene. It is found that the bond length of C-C in the graphene system is about 1.42 Å, which is consistent with the experimental result (1.415 Å). The binding energy of graphene-H is reported to be 0.83 eV in the literature.

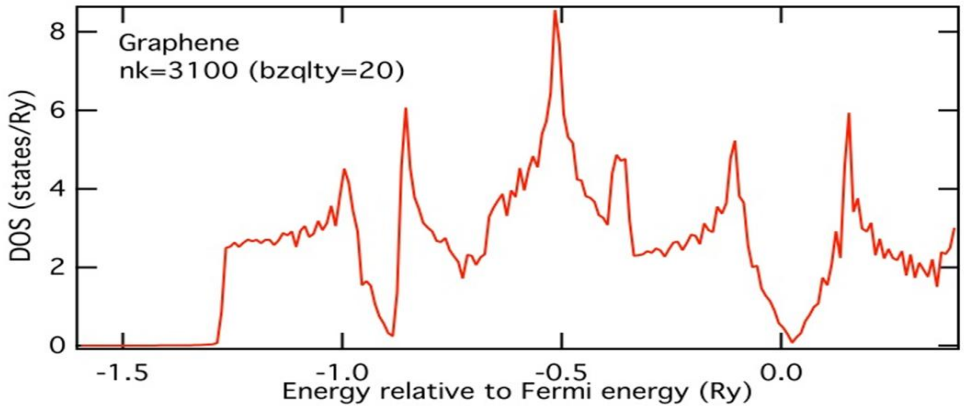

Figure 2: Density of states of pure graphene.

The density of states of pure grapheme was calculated and shown in Figure 2. The conduction and the valence bands cross at the Fermi level. It is quite obvious that the states around Fermi level belongs to C-p_z orbitals since the graphene is located in x-y direction.

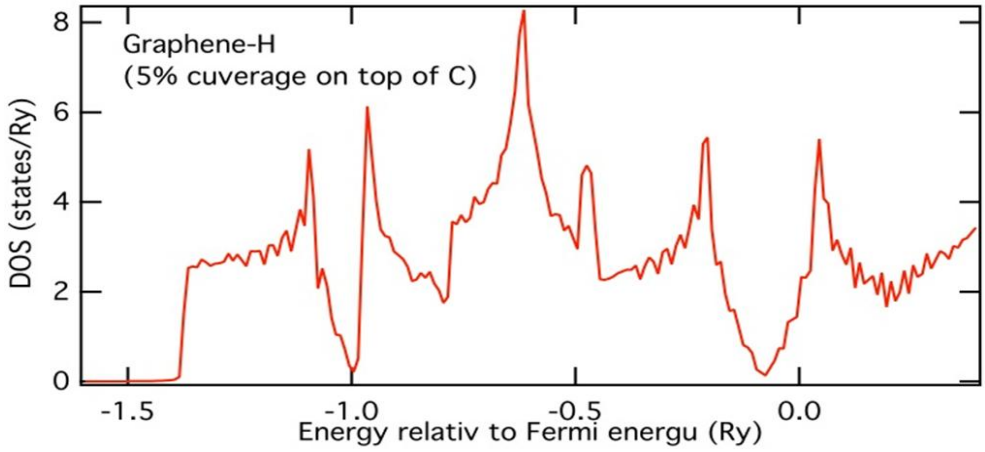

Figure 3: Density of states of graphene with adsorbed H (5% H coverage).

The Fermi level of a graphene with hydrogen on top (5% hydrogen coverage) is shifted upward. This means that the system is n-doped. For these cases, the original shape of the graphene presents only small deviations from the pristine form. Therefore the grapheme is slightly distorted ue to the dopant.

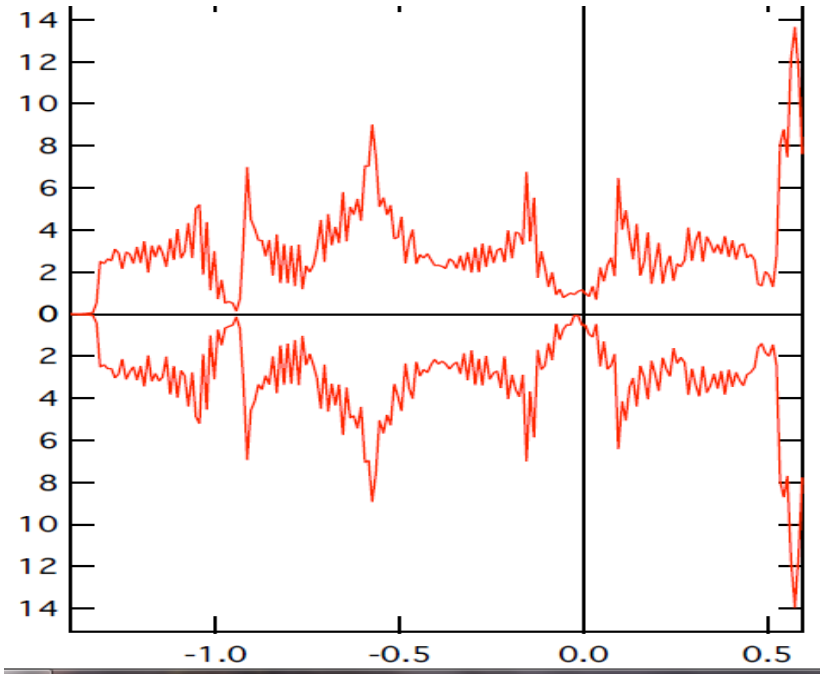

Figure 4: Density of states of grapheme with adsorbed H (5%H coverage) with consideration of the magnetic property.

Figure 4 shows the spin polarized density of states of grapheme with H adatom (5%H coverage). It shows the characteristic feature of a half-metal. That is, metallic in spin-up band but semiconductor for spin-down band. This happens because the adsorbed hydrogen breaks the phi bonding of carbon's p_z orbitals.

5. Conclusion

The hydrogen impurity causes the Fermi level of graphene to shift. 5% hydrogen coverage on top site of an infinite graphene sheet makes graphene become half-metal ferromagnetic. This property is useful in the field of spintronics.

6. References

1. K. S. Choi, C. H. Park, J. Korean Phys. Soc. 54 939 (2009)
2. N. Park, S . Lim, G. Kim, J. Korean Phys. Soc. 53 691 (2008)
3. T. A. Nugraha, et al, Indonesian Journal of Physics. 21 1 (2010)

My Japan Life Experience

I came to Japan to attend the QED Short Term program. It is my first experience go to abroad from Indonesia. When I arrived at Kansai airport I was really surprised because Japan is very clean. I remember seeing a train conductor when conductors come in to check tickets. He walked in front of me then bowed his head and repeat it before he leaves. He really did it right and bowed slowly. Frankly, I was so impressed by the politeness of the Japanese people. It took some months to get accustomed to the new environment, culture and hard work. I am so happy that I became a short term student because I got a chance to study computational material design, to attend some lectures, workshops and Japanese classes. It was fabulous!

Nagano is one of the places I have been to. With many indonesian friends, I went to Nagano to play skiing It really is my first experience to see snow. It could be the best snow I ever seen. Awesome!

My first day in skiing was spent at Ngano prefecture. I rode the gondola up. At first, skiing is so difficulty. I tried to practice, practice and practice. I learned how to stop my glide. I turned the front portions of skis slightly inward. I did not accelerate too fast in first runs. Then I gained experience in increasing and decreasing my speed. Finally, I manage to control my speed naturally by moving my ski in maneuvering the V position. Ovations!

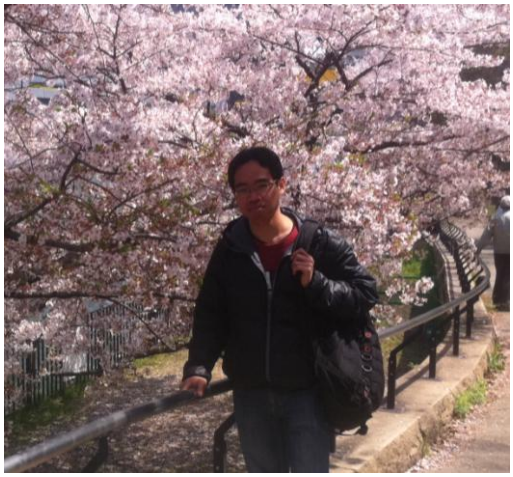

Spring came and the cherry blossoms were in bloom. I went to Osaka Jo Kouen to enjoy the hanami. In the mainland, the trees are in bloom. People with cameras in hand captured the beautiful cherry blossoms. The sakura, which blooms suddenly and beautifully only blooms for a period of a couple of days and then falls to the ground. Many people gather to do picnics, eat and drink under the cherry blossoms. It is one of the most beautiful times of the year in Japan and definitely worth trying for. “Off the hook ”!

I would like to extend my deepest gratitude and thanks to Prof. Hisazumi Akai for the Trust and Overwhelming support.

In conclusion, I want to say “thank you” from the bottom of my heart to Prof. Hisazumi Akai, Prof. Hideaki Kasai, Dr. Masako Ogura, Ms. Tomoko Shimokomaki, Ms. Reiko Tanaka, Ms. Ikuko Nojiri. I hope that one day we would meet again, maybe in Japan or even Indonesia.

Gagus Ketut Sunnardiano
Indonesia

STRUCTURAL STUDY OF α -TETRAGONAL BORON BY COMPUTATIONAL METHOD

Jagadeesh S, N Uemura, K Shirai

Nanoscience and Nanotechnology Center, ISIR, Osaka University, Japan

Abstract

In this work, we investigated the formation of α-Tetragonal boron phase and the electronic structure by first-principles pseudopotential method for bulk crystal. Enthalpy of formation (ΔH_f) and phonon calculation utilized as the tool for determine the real structure of α-Tetragonal boron.

1. INTRODUCTION:

Boron is a unique element with structural complexity. It belongs to III-B group. It is a trivalent element and tendency to form directional chemical bond. The trivalent elements form usually metallic bonds and are electron deficient for usual covalent bonding, boron forms unique three-centered covalent bond that induce several icosahedral cluster based crystalline structures. The Crystalline boron exists as several polymorphs, α and β Rhombohedral, α and β Tetragonal. Among them the α-Tetragonal boron attracts attention from researchers due to its structural uniqueness, that is, a tetrahedral arrangement of icosahedra. The α-Tetragonal boron synthesized by Laubengayer *et al*[1] in 1943. It seems to be six decades old, but still it is a hot topic in the material research due to its bonding nature and structure. In the history of boron research, the α-Tetragonal boron phase has been occupying a special position to shade the nature of icosahedral bonding.

Debate on α-tetragonal boron structure:

Initially, it was thought the crystal is composed of four B_{12} (12 boron atoms) and two interstitial atoms, being 50 atoms in the cell. The synthesis of α-Tetragonal boron was first reported in 1943 by Laubengayer *et al*[1]. This proposed structure was suspected by Longuet-Higgins *et al*[2] in 1955 using theoretical calculation method. In 1958, the single crystal α-Tetragonal boron was synthesized by Hoard *et al*[3], They concluded that the B_{50} structure existed (supported to the Laubengayer work). The α-Tetragonal boron was synthesized with impurity elements like C (Carbon) and N (Nitrogen) by Amberger *et al*[4] in 1971. They proposed that the pure B_{50} structure is not possible, it should be $B_{50}+X_2$, where X= C, N, and B. Seongbok Lee *et al*[5] supported this work in 1992 by first principles calculation method.

However, as the structural refinement was progressed, it become clear that pure B_{50} structure alone was unstable. Impurities such as C or N atoms are incorporated in the crystal and only in the form of α-Tetragonal phase can be stabilized. A recent surprise that, pure B_{50} form is reported in nanostructure boron,

such as nanoribbon[6], nanobelt. There is no consensus regarding the stability of α-Tetragonal phase in nanostructure[7].

Issues:

Does α-Tetragonal boron structure contain only B_{50} atoms? What is the reason behind in the formation of pure B_{50} form only in nanostructure boron? How the multi structure nanomaterials arises?
To figure out these issues, one must consider the real structural study of bulk crystal of α-Tetragonal boron. Then one can study about the nanostructure of the α-Tetragonal boron.

2. STRUCTURE AND BONDING:

The boron element belongs to III-B group in the periodic table. The atomic number is five. So it has $1s^2 2s^2 2p^1$ electronic configuration. It contains three valence electrons in four available orbitals and most of its compounds have covalent and multi center type bonds rather than ionic and / or metallic bonds. These types of bonding together occurring in electron deficient compounds. The basic unit of the α-Tetragonal boron structure is icosahedra. The α-Tetragonal boron structure contains four icosahedral unit and two interstitial atoms.

Icosahedral unit:

An icosahedral unit contains 12 vertexes, 20 faces and 30 edges (Fig 1). The each vertex occupied by 12 boron atoms. A boron atom at vertexes can make five equal bonds to its nearest neighbors. Thus in terms of conventional bonding, each boron atoms must supply five electrons toward the creation of bonds to each of five neighboring atoms in icosahedron. However each boron atom has no more than three valence electrons. Indeed, some electron required for bonding among icosahedra. So that it is impossible to interpret the structure in terms of ordinary rules of covalency. With in each icosahedron there are at most 36 (12B×3e) electrons available for bonding. On the other hand each atom provides 48 (12B×4) bonding orbitals. It can be refer as *electron deficient or half bond* structure[8]. A key element to understanding the electron deficient bonding with in boron icosahedra is the *three-center bond*. The charge density study showed that the charge located on the center of the triangle (face of icosahedral unit).

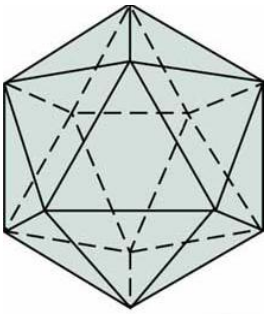

Fig 1

Structure of α-Tetragonal boron:

The structure belongs to $P4_2$ / n n m space group. The unit cell consisted of two B atoms at (0,0,0) and (1/2,1/2,1/2) and four icosahedra centered at (1/4, 1/4,1/4) ,(3/4,3/4,1/4),(1/4,3/4,3/4),(3/4, 1/4,3/4) resulting in a unit cell B_{50} atoms. It has the typical tetragonal structure, the c (4.928Å) axis shorter than the a,b (8.655 Å) axes. It has tetrahedral arrangement of icosahedra as seen in following figure.2. It has a large number of interstitial voids. It could be accommodate additional boron atoms as well as impurity atoms.

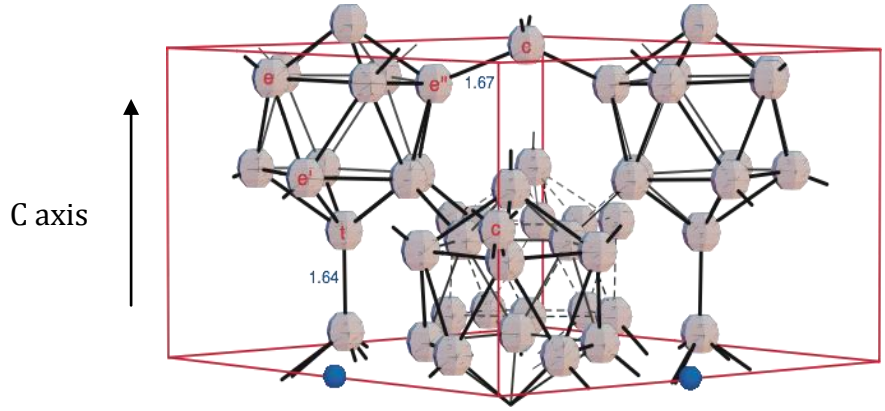

Fig 2

In this structure, blue colored sphere refer to the possible location of the impurities atoms like C, N and B. The icosahedra connected with inter and intra half bond. The general formula of the structure is $4\ B_{12} + B_2 + X_2$, Where X = C, N and B.

3. METHODS AND DISCUSSION:

Electronic-structural calculations were performed by the first principles pseudopotential method. The code used was **'Osaka2002'**. Troullier-Martins pseudopotentials were used, with the aid of a full separable Kleinman-Bylander form. The plane wave basis was used for expanding the wave function. The cut-off energy E_{cutt} of 20 Ry was used for this calculation. The calculation results are mainly based on LDA (Local Density Approximation) method.

Calculation of enthalpy of formation (ΔH_f):

The enthalpy of formation of various defects with respect to pure α-Tetragonal boron phase was calculated. The results are given below in Table 1. The ΔH_f of the B_{50} is too high compare to other compounds, which contains impurity atom. It showed that the formation of the pure B_{50} form is unstable. On the other hand formation of $B_{50}N_2$ and $B_{50}B_2$ is possible with low formation energy. We concluded from this calculation of enthalpy of formation is the pure B_{50} form is unstable.

Compound	ΔH_f (eV /atom)	Ref.states
B_{50}	0.122	α-B
$B_{50}C_2$	0.024	α-B+dia
$B_{50}N_2$	**-0.054**	α-B+N_2 mole
$B_{50}B_2$	**-0.071**	α-B+tetra

Table 1

Calculation of bond length:

The bond length was calculated between various boron atoms located in icosahedra and interstitial site. The result was listed in the Table 2, the bond lengths were stated in Å. The obtained result was compared with the experimental value. The calculated lattice parameter (a,b,c axis) value is slightly lower than the experimental value. Where, e –equilateral boron atom, c-center boron atom, t-top site boron atom and i-inter icosahedral bond (Fig 3).

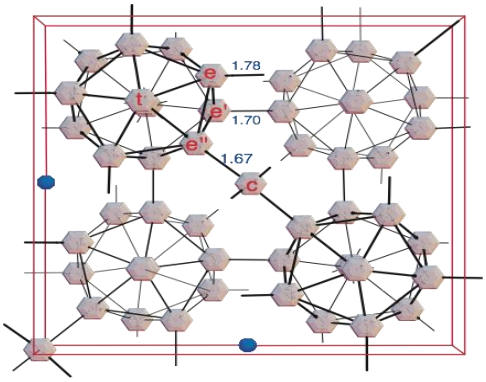

Fig 3 (Top view of the structure)

We observed the common phenomenon, which is arise in other boron rich icosahedral crystals, that is *inter*icosahedra bond length is shorter than the *intra*icosahedra bond lengths. The nature of bonding of B_{12} was illustrated many years ago in terms of MO theory. The strong *inter*icosahedra bond reveals that it has high covalency character than the (three-center or half bond) *intra*icosahedra bond. The researcher claim that this kind of material as 'inverted molecular solid'[8].

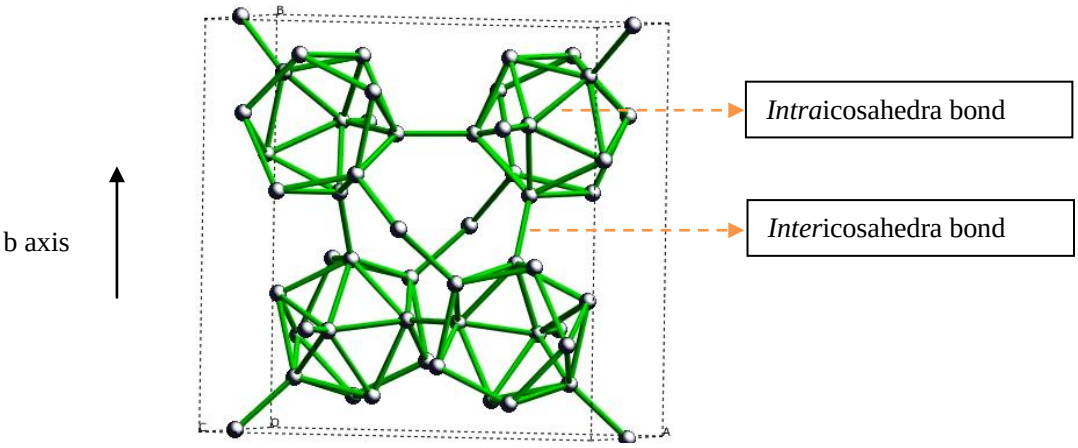

Fig 4 (Front view of the structure)

	α-tetra	(exp)	+C_2	+N_2	(exp)	+B_2
a	8.65865	8.75301	8.68155	8.66250	8.643	8.73379
C	4.92849	5.0930	4.97963	5.02592	5.128	4.97567
V/N	7.3900		7.2175	7.2527		7.2988
t-t	1.6439		1.6423	1.6574		1.6447
e-e	1.7838		1.7041	1.6608		1.7515
e'-e'	1.6995		1.6367	1.6490		1.6533
e"-c	1.6702		1.6341	1.6115		1.6787
i-e			1.6884	1.6143		1.7895
intra	1.7634		1.7679	1.7712		1.7745

Table 2

Phonon spectrum:

The phonon calculation is one of the right tools to determine the material properties. The phonon spectrum was obtained by frozen phonon calculation.

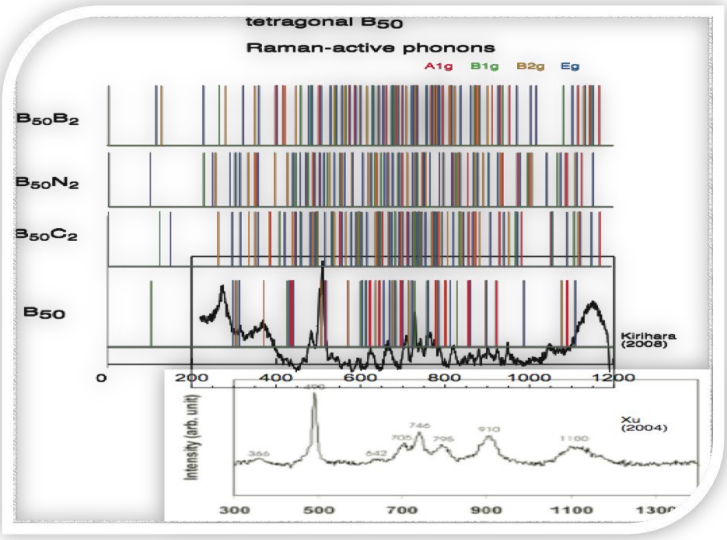

Fig 4

The various vibration modes of various boron compounds are showed in the spectrum (Fig 4). Distinguishing the various modes in this spectrum is quite complicated process. The Raman and IR spectrum was coincided with the calculated value, which is shown in the above spectrum. The incorporation of foreign atoms like C, N and B enhanced the strength of the *inter*icosahedra bond. It means that the interstitial sites play a crucial role on the stability of crystal.

4. SUMMARY AND CONCLUSION:

In this work, we investigated the formation of α-tetragonal phase and the electronic structure by first-principles pseudopotential method for bulk crystal. The enthalpy of formation (ΔH_f) of various defects with respect to pure α-tetragonal phase revealed that the pure B_{50} structure is unstable. As commonly observed in other boron crystals, the intericosahedra bond lengths are shorter than the intraicosahedra bond lengths. It means that the interstitial sites play a crucial role on the stability of crystal. Phonon calculation of the α-tetragonal boron confirmed the strong bonding between two icosahedra units. We observed the characteristic phenomenon, when the foreign atoms are incorporated in this structure. The phonon spectrum showed, the inter icosahedra bond strength enhanced by the foreign atoms like C, N and B.

5. ACKNOWLEDGMENT:

My sincere thanks to **Prof. Hideaki Kasai** for given this wonderful opportunity. At the very onset I would like to express my deep sense of gratitude to **Assoc.Prof. Koun Shirai**, my supervisor for permitting me to work in his esteemed laboratory and his dynamic guidance throughout the project work. It is colossal opportunity to expose myself to the research environment of Osaka University, Japan.

My special thanks to my lab members Prof. Yanase A, Prof. Oguchi T, Assi.Prof Yamauchi K, Mrs. Kakiuchi M, Mr. Fujimura T, Mr. Uemura N and Mr. Tanaka Y for their constant encouragement and moral support that I have received all through my project. Finally I would like to thank my beloved parents, because of all their efforts I am successfully standing here. I am thankful to my brother for his precious help and moral support. My special thanks go to my friends and family members for their blessings and well wishes. Last but not least, my sincere thanks to all staff members and students of QEDC.

6. REFERENCES

1. Laubengayer et al, J.Am.Chem.Soc, 65, 1924, 1943.
2. H.C. Longuet-Higgins et al, Proc.R.Soc.London, Ser.A, 230,110,1955.
3. J.L Hoard et al, J.Am.Chem.Soc, 80, 4507, 1958.
4. E. Amberger et al, J.Less.Common.Met, 23, 21, 1971.
5. S.Lee et al, Phy.Rev B, 45, 3248, 1992.
6. Wang et al, Chem.Phy.Let, 368, 663, 2003.
7. Wataru Hayami et al, J.Phys.Chem.C, 111, 688, 2007.
8. David Emin, J.Solid Stat.Chem, 179,2791,2006.

LIFE AS A SHORT TERM STUDENT IN OSAKA UNIVERSITY

By

Jagadeesh S

It is a great pleasure to me to share my experience as a short term student in Osaka University, Japan. I arrived in Japan on 28 Sep 2010. I have been staying in Osaka University international student dormitory for almost eleven months. I remembered my first three days in Japan; it was the longest day and night in my life. I was home sick at that time. After that it was like my dream world, I enjoyed so much in whole period of my course.

As an experimentalist, I struggled a lot to solve the problems that arose in theoretical field but I enthused to do research in computational field. Honestly speaking, it was like walking through a dark forest during first three months. My sensei (supervisor) helped a lot to overcome my problem. I am fortunate to have such a friendly professor and lab members. I attended some regular classes with Japanese students, who helped to understand the subject. The days are running like the wind, my research also progressed and completed the project in best level.

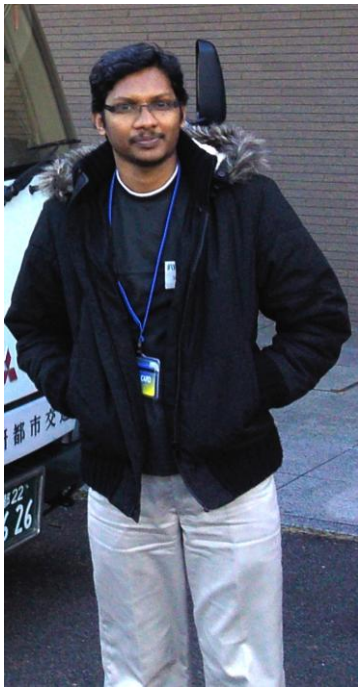

Apart from study, I have enjoyed my life as a normal human being. I met various people from various countries. We lived together in the dormitory and shared our real customs and cultures. We arranged a various party and some time I visited other dormitory, it means I did not make boundary to make a good friendship. I visited some of my Japanese friend's home. It helped a lot to know about the Japanese culture. My Japanese friends helped a lot to overcome my daily life activity problem, like transportation, purchase, interact with other social bodies and etc.

I can't forget about CMD workshop, which is my first workshop in Japan. I attended the workshop with my friends and enjoy the pleasant location in Kyoto. At the same time, I felt the tremors on 11-04-2011. I visited many place in and around Osaka for past eleven months. My first visited site was Kyoto. I went to many shrines; I was amazing about the construction of the shrine. Then I went to Osaka Aquarium, Osaka Castle, Osaka sky building, Universal studio, etc. I met some of foreigners during my visit. My journey is not end, I will present my research work in forthcoming conference, which is held in Tokyo, Hope I will have good time.

It is not hard to adapt the Japan climate, food and other customs. This is the wonderful opportunity for me as a QED short term student at Osaka University, Japan. If you ask me in a one word about my life in Japan. The answer is *awesome, awesome, and awesome.*

Thank You All

The study of adsorption of molecular oxygen on single-walled carbon nanotubes (SWNTs) for gas sensor.

Muhammad Aslam Rosle

Kasai Laboratory, Department of Applied Physics, Graduate School of Engineering
Osaka University, 565-0871, JAPAN

Abstract

Single-walled carbon nanotubes (SWCNTs) have been attracting great interest for their unique physical and chemical properties. Carbon nanotubes (CNTs), which are known as rolled-up graphene sheets of carbon, are one of the most promising molecular structures for a wide range of future technological innovations. In particular, because of size, large surface area, and hollow geometry, CNTs are being considered as prime materials for gas adsorption [1]. There is a strong interest in gas adsorption by carbon nanotubes. Some physicists have discovered that exposure to O_2, NO_2 or NH_3 dramatically influences the electrical resistance and thermoelectric power of semi-conducting SWCNTs [2]. The utilization of these properties has led to application of gas sensors. In this regards, the gas adsorption has a significant effect on the electronic structure of the SWNTs which is determined by chirality and diameter. Among other gas, oxygen is one of the important molecules that play essential roles in many aspects of SWCNTs. Therefore, this research is endeavored to investigate the effect of molecular oxygen adsorption on the geometries and electronic properties of small and large armchair single-walled carbon nanotubes (SWCNTs) by means of the density functional theory (DFT). The investigation also focuses on the physisorption and chemisorptions of molecular oxygen.

INTRODUCTION

In recent years, carbon nanotubes (CNTs) are getting prominent among researchers due to their importance as building blocks in nanotechnology. The special geometry and unique properties of carbon nanotubes broaden great potential applications including nanoelectronic devices, energy storage, chemical probes and biosensors, field emission display, etc [1–4].

In particular, gas adsorption in carbon nanotubes is an important issue for both fundamental research and technical application of nanotubes. Having a bright potential in terms of size, large surface area, and hollow geometry, carbon nanotubes are being considered as prime materials for gas adsorption. So, the effect of gas environment on the electronic properties of carbon nanotubes has recently attracted a great deal of attention [5–11].

Based on past researches, the electrical conductance of the semiconducting tubes is dramatically changed whenever O_2, NO_2, or NH_3 gas is exposed [6,12]. In other words, the electronic properties of carbon single-wall nanotubes (SWNTs) can be appreciably altered by the presence of adsorbed molecules. This significant behaviour has led to considerable interest in the possible use of SWNT's as the basis of chemical or gas sensors.

In general, the gas detection principle is a change in electrical property of detecting material upon exposure to the gas. Therefore, the effects of gas adsorption, especially O_2 adsorption on the SWCNTs have intensively investigated. In this matter, oxygen has been found to influence electronic properties of SWNTs, with the electrical resistance, the thermoelectric power, and the local density of states [1]. The increased electrical conductivity induced by oxygen adsorption has been attributed to an increase in the local density of states and a shrinking of the band gap of the nanotube.

There are several mechanisms may explain adsorption phenomena on SWCNTs. The gas molecules could affect transport properties indirectly, which by binding to donor or acceptor centers in the substrates or at the contacts; or directly, by binding to the nanotube [10]. In latter case, the gas could be physisorbed (bound by dispersive van der Waals forces) or chemisorbed (bound by formation of a chemical bond). If the gas is chemisorbed, a key factor affecting the transport properties would be the charge transfer from the gas molecule to the nanotube, or vice versa.

Therefore, this research is aimed to study the physisorption and chemisorptions by using density functional calculations with Vienna Ab-initio Simulation Package (VASP) application for adsorption of oxygen molecules on a SWCNT.

The objectives of this research are:

1. To investigate the effects of the molecular oxygen adsorptions on the stability of tubes.
2. To identify the best chirality for the best candidate of pristine SWCNTs gas sensor.
3. To understand the adsorption reaction of molecular oxygen behaviours at various sites for different tubes.

In fact, sensing gas molecules is critical to environmental monitoring, chemical control processes, agricultural, space missions and medical applications. Currently, the gas sensors have widely been using semiconducting oxides such as ZnO, SnO_2 and In_2O_3 [13]. However, this kind of gas sensing material put a limit on the size and geometry of sensor due to necessity being governed by the micro fabrication technique.

Fortunately, the discover of CNTs brings the bright future path for being the best selection of gas sensing material due to small size (diameter ≈1-100nm), good electrical and mechanical properties as well the most promising factor that has high specific surface area (1580 m^2/g). Since the CNTs possess extremely high surface-to-volume ratio and hollow structure of nanomaterials,

it is reported as ideal for gas molecules adsorption and storage [14,15]. Therefore, this research is highly motivated to the innovation of oxygen sensors based on carbon nanotubes (CNTs) to attain the sustainability of being useful technology.

For instance, the CNT-based oxygen sensors are important as safety devices which they are useful in confined spaces such as mines vessels and aircrafts. Besides, it can be applied for environmental monitoring such as leakage detection and some chemical manufacturing process. Moreover, the development of CNT-based oxygen sensors is believed to be significant technologies for space discoveries in the future.

COMPUTATIONAL DETAILS

The adsorption of oxygen molecule on SWNTs is performed using a plane-wave pseudopotential method with generalized gradient approximation (GGA) correction of exchange-correlation energy and energy cutoff is set to 600eV for calculating total energy.

Meanwhile, the Brillouin zone is sampled with 1X7X1 Monkhorst meshes whereas k-points are sampled on a uniform grid along the tube axis and atomic positions are fully relaxed.

In this investigation, the diameters of 4Å SWCNTs are utilized. Thus, three different types of 4Å tubes are identified as zigzag (5,0) tube, armchair (3,3) tube and chiral (4,2) tube. On the other hand, total energy of the oxygen molecule with bond length of 1.24Å is calculated using spin-polarization. To examine the binding properties of these tubes, the adsorption energy E_a (d) is defined as the total energy gained by molecule adsorption at equilibrium distance [16] :

$$\mathbf{E_a(d) = E_{tot}(tube + O_2 molecule) - E_{tot}(tube) - E_{tot}(O_2 molecule)}$$

Where E_{tot}(tube + O_2 molecule) corresponds to the energy of the tube adsorbed with O_2, E_{tot}(tube) is the energy of the isolated tube, and E_{tot}(O_2molecule) is the energy of the singlet O_2 molecule.

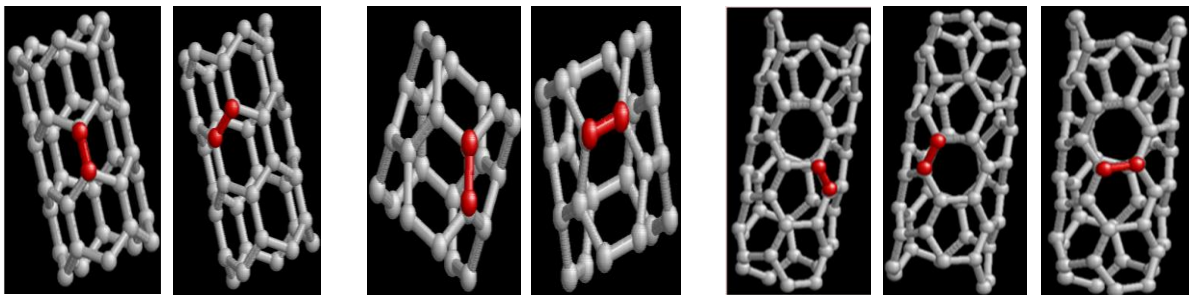

a) (5,0) at site I (Left) Site II (Right)

b) (3,3) at site I (Left) Site II (Right)

c) (4,2) at Site I (Left), Site II (Middle) and Site III (Right)

Figure 1: Distinct adsorption sites of molecular oxygen on the outer tube surface

In this regard, the calculation is conducted by Vienna Ab-initio Simulation Package (VASP).

RESULT AND DISCUSSION

In this investigation, the molecular oxygen adsorption is performed on the outer surface of 4Å tubes. For tubes (5,0) and (3,3), there are basically two distinct adsorption sites, in which site I is related to molecular oxygen with carbon-carbon bonds along tube axis whereas site II associated with the bonds that around tube circumference. Meanwhile, chiral (4,2) tube identified as 3 different adsorption sites by considering site I,II and III for smallest, larger and largest angle with tube axis.

3.1 Adsorption Analysis of Zigzag (5,0) Tube

Based on fig. 2 and 4, both graphs show the physisorption of oxygen occur on both sites but the binding very weak. The data tables 1-3 also show the O-O distance and tube geometry in physisorption are almost unchanged.

Tube (5,0)	E_b (eV)
Physisorption (site I)	-0.05
Physisorption (site II)	-0.15
Chemisorption (site I)	-1.55
Chemisorption A (Site II)	-0.85
Chemisorption B (Site II)	-3.11

Table1: Calculated binding energy (in unit of eV) for O_2 adsorbed on tube (5,0).

As chemisorption occur at site I, the study show that the C-O bonds formed "square" ring between O_2 and tube. Due to strong interaction between O_2 and tube, the C-C bonds were elongated about 0.1 Å but tube geometry is still kept. On the other hand, Site II is observed to have the chemisorbed product which could go another step to be more stable without dissociation of oxygen. Therefore, the analysis of (5,0) suggests that site II has stronger interaction (physisorption & chemisorptions) than site I and on both sites the their tube geometry can be successfully maintained.

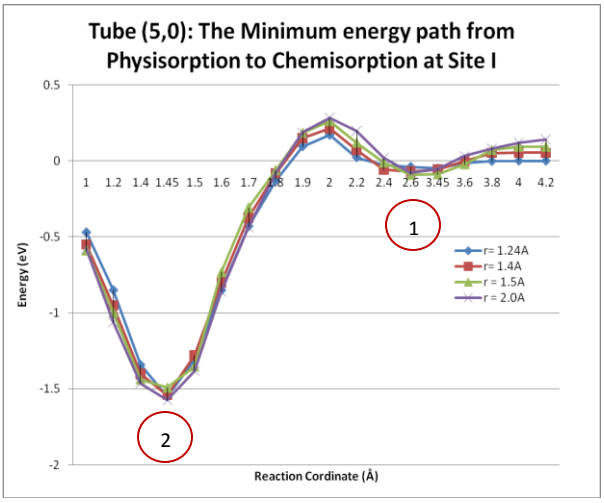

Figure 2: The minimum energy path from physisorption at site I to the chemisorptions on tube (5,0).

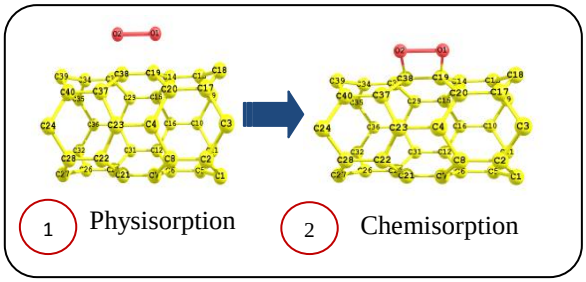

Figure 3: The molecular pictures involved in reaction paths on site I of tube (5,0).

Physical Parameters	Physisorption State	Chemisorption State
O-O Length (Å)	1.247	1.505
C- C Length (Å)	1.421	1.520
C-O Distance (Å)	3.450	1.450
Activation Energy	ΔE_A = 0.22eV	

Table 2: Calculated structural parameters for physisorption and chemisorptions states in (5,0) tube at site I.

Physical Parameter	Physisorption State	Chemisorption State	
		A	B
O-O (Å)	1.255	1.515	3.016
C- C (Å)	1.424	1.451	1.473
C-O (Å)	3.450	1.900	1.450
Activation Energy (eV)	ΔE_B = 0.25eV		ΔE_C = 0.45eV

Table 3: Calculated structural parameters for physisorption and chemisorptions states in (5,0) tube at site II.

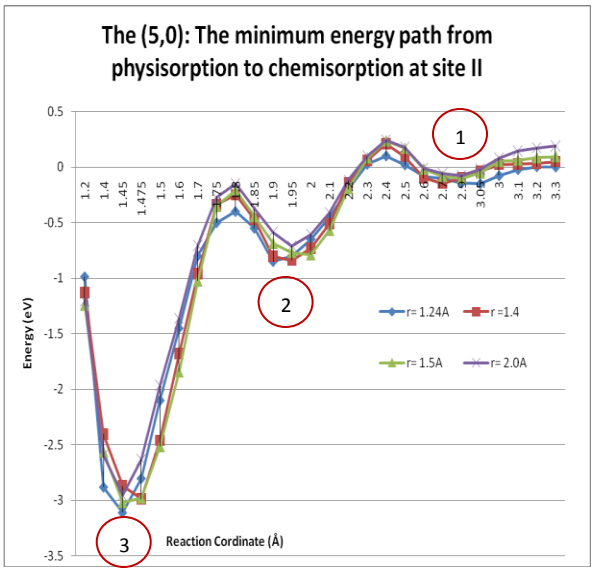

Figure 4: The minimum energy path from physisorption at site II to the chemisorptions on tube (5, 0).

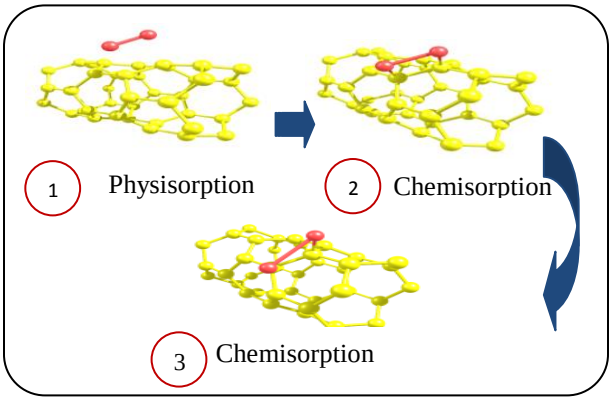

Figure 5: The molecular pictures involved in reaction paths on site II of tube (5,0).

a) Adsorption Analysis of Armchair (3,3) Tube

For adsorption analysis tube (3,3), the physisorption for both sites observed the O-O bond length slightly larger than free oxygen molecules. As chemisorptions occur, both sites experience dramatic change of tube's geometry and strong interaction due to largest curvature of C-C bond among 3 types 4Å tubes. At site I, the C-C bond was broken and oxygen elongated. Meanwhile, site II experience several terminals of chemisorptions where initially C-C bond and O-O bond elongated and further attraction between O_2 and tube resulting C-C bond broken. Gradually, this continuous elongated molecular oxygen finally dissociated.

Hence, the analysis (3, 3) tube suggests its chemisorptions interaction for both sites are stronger than tube (5,0). In this particular, site II has stronger adsorption energy than site I among tube (3,3). However, the stability of the tube (3,3) is weaker than (5,0) due to both sites experience destruction of C-C bond of tube. Besides, although site II shows dissociation oxygen occurs at last terminal, the activation energy which oxygen need to be dissociated is extremely high so the study suggests oxygen is not possible to be dissociated on both sites.

Tube (3,3)	E_b (eV)
Physisorption (site I)	-0.24
Physisorption (site II)	-0.28
Chemisorption (site I)	-3.28
Chemisorption (Site II)	-0.93
C-C Bond Broken (Site II)	-2.46
O_2 Dissociated (Site II)	-4.10

Table 4: Calculated binding energy (in unit of eV) for O_2 adsorbed on tube (3,3).

Physical Parameters	Physisorption State	Chemisorption State
O-O Length (Å)	1.268	2.373
C- C Length (Å)	1.480	1.511
C-O Distance (Å)	2.507	1.210
Activation Energy (eV)	ΔE_A = 0.27eV	

Table 5: Calculated structural parameters for physisorption and chemisorptions states in (3,3) tube at site I.

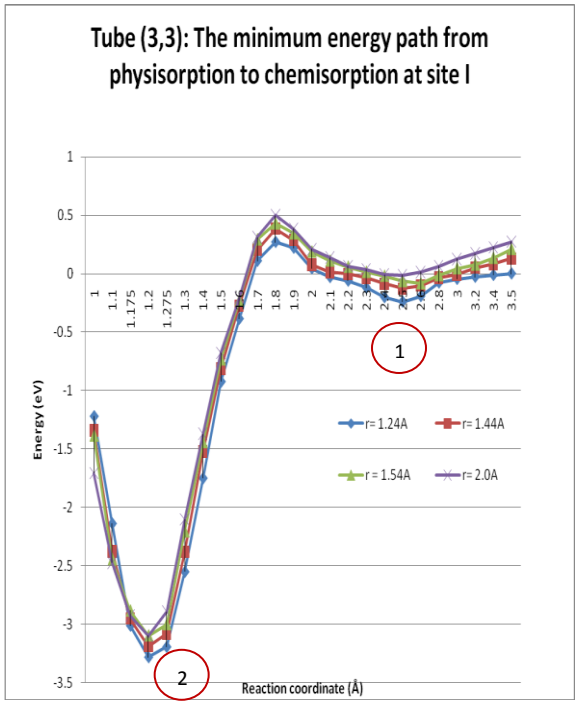

Figure 6: The minimum energy path from physisorption at site I to the chemisorptions on tube (3,3).

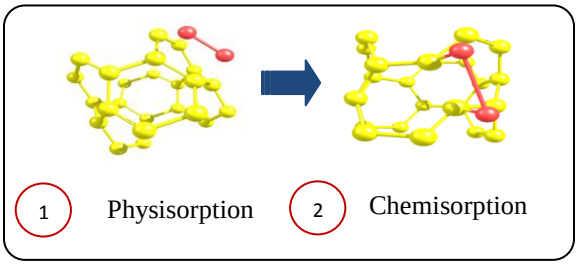

Figure 7: The molecular pictures involved in reaction paths on site I of tube (3,3).

Physical Param.	Physis. State	Chem. State	C-C Bond Broken	O_2 Dissoc.
O-O (Å)	1.271	1.503	1.972	2.570
C- C (Å)	1.449	1.452	1.580	1.611
C-O (Å)	3.35	2.10	1.825	1.400
Barrier Energy (eV)	ΔE_B = 0.19eV	ΔE_C = 0.42eV	ΔE_D = 1.91eV	

Table 6: Calculated structural parameters for physisorption and chemisorptions states in (5,0) tube at site II.

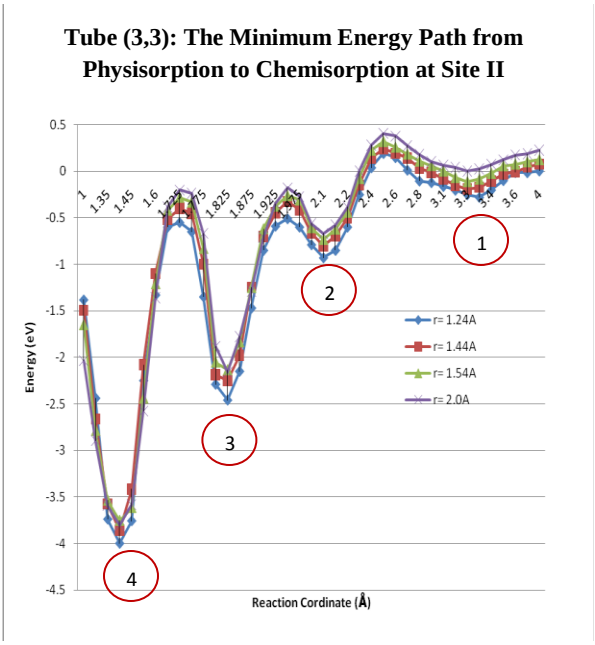

Figure 8: The minimum energy path from physisorption at site II to the chemisorptions on tube (3,3).

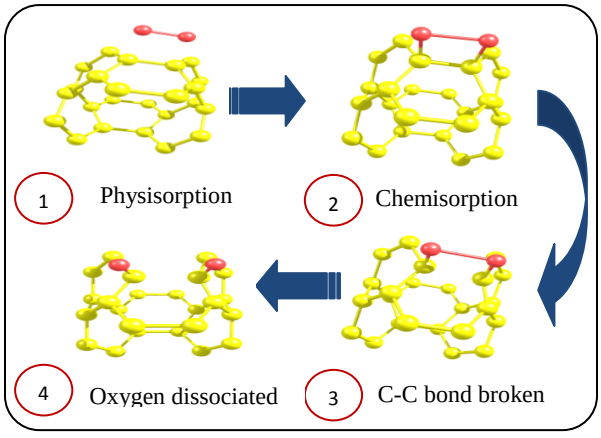

Figure 9: The molecular pictures involved in reaction paths on site II of tube (3,3).

b) Adsorption Analysis of Chiral (4,2) Tube

Based on the calculated results, the adsorption of oxygen on CNT (4,2) at site III shows the lowest energy barrier for transition between physisorption and chemisorptions state among other adsorption sites of (4,2) tube with oxygen. This findings imply that adsorption at site III is preferable and occurs upon oxygen exposure on the (4,2) tube since it only consume the most minimum energy (barrier energy) to interact between oxygen adsorbate and tube.

After undergoing chemisorptions, the site III recorded as the strongest binding energy among other sites of (4,2) tube. This finding suggests that due to curvature effect, site III is the most reactive. Comparatively, site I and site II both have C-C bonds elongated but site II displays larger C-C bond than site I since it is more reactive. Unfortunately, for adsorption site III, once chemisorptions process is through, the (4,2) tube is observed to no longer possess CNT since characteristics of C-C bond was broken and tube's geometry was significantly changed. So, the (4,2) tube is not good candidate for gas sensing material due to failure to maintain geometry.

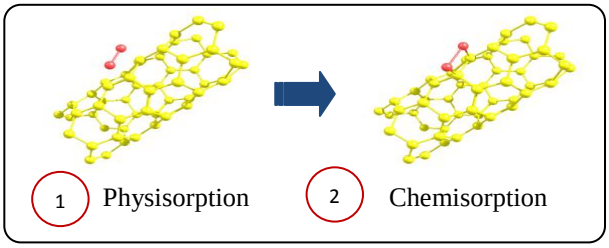

Figure 10: The molecular pictures involved in reaction paths on site I of tube (4,2).

Tube (4,2)	E_b (eV)
Physisorption (site I)	-0.15
Physisorption (site II)	-0.27
Physisorption (site III)	-0.15
Chemisorption (site I)	-1.25
Chemisorption (site II)	-0.75
Chemisorption (site III)	-3.20

Table 7: Calculated binding energy (in unit of eV) for O_2 adsorbed on tube (4,2).

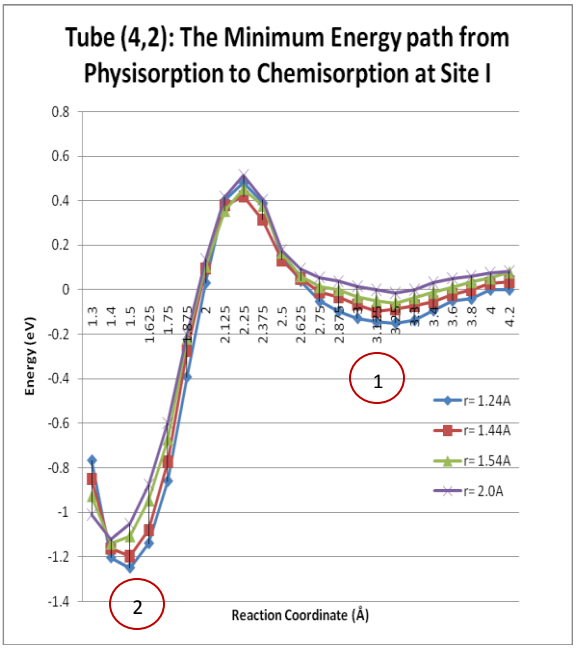

Figure 11: The minimum energy path from physisorption at site I to the chemisorptions on tube (4,2).

Physical Parameters	Physisorption State			Chemisorption State		
	Site I	Site II	Site III	Site I	Site II	Site III
O-O Length (Å)	1.250	1.247	1.258	1.550	1.560	2.705
C- C Length (Å)	1.443	1.431	1.425	1.478	1.492	1.510
C-O Distance (Å)	3.250	2.850	3.125	1.530	1.500	1.250
Activation Energy/ Barrier Energy (eV)	ΔE_A = 0.63eV ΔE_B = 0.50eV ΔE_C = 0.44eV					

Table 8: Calculated structural parameters for physisorption and chemisorptions states in (4,2) tube at respective adsorption sites.

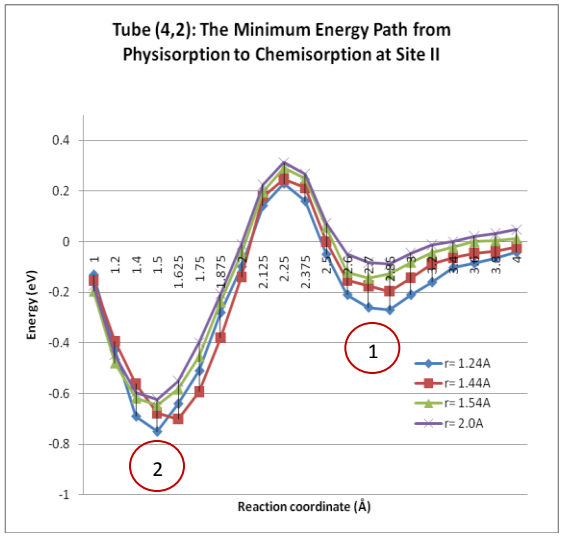

Figure 12: The minimum energy path from physisorption at site II to the chemisorptions on tube (4,2).

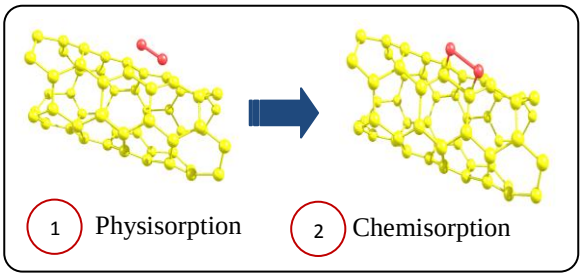

Figure 13: The molecular pictures involved in reaction paths on site II of tube (4,2).

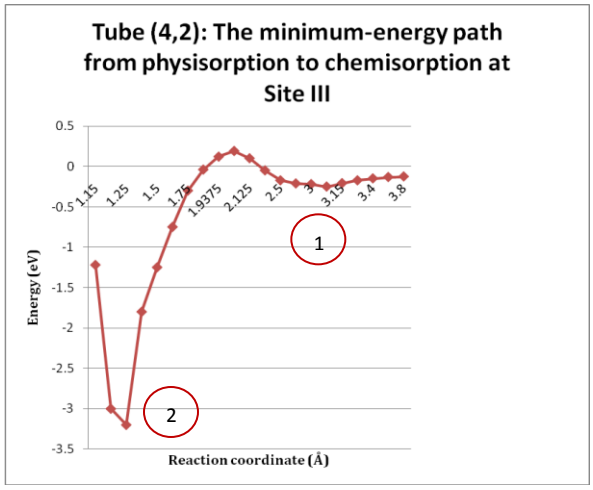

Figure 14: The minimum energy path from physisorption at site III to the chemisorptions on tube (4,2).

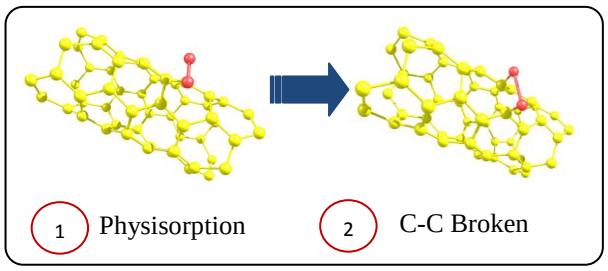

Figure 15: The molecular pictures involved in reaction paths on site II of tube (4,2).

SUMMARY

In summary, the interaction of molecular oxygen with 4Å Single-Walled Carbon Nanotubes (SWCNTs) which consist of different chirality have proven to play important role in oxygen binding energy and reaction process. As a whole, the study analysis suggest that (5,0) tube as the most stable and the best candidate for gas sensing material rather than (3,3) and (4,2) tube due to excellent property of keeping up its geometry without breaking the C-C bond structure for all sites (only smallest change of C-C bond upon adsorption which recorded at ±0.1Å) as well as strong binding energy of chemisorptions. In contrary, the (4,2) and (3,3) tubes fail to maintain their tube geometry despite of strong interaction occur. Some of their sites are observed to be no longer "CNT" since their characteristic possess a broken C-C bond.

ACKNOWLEDGEMENT

Firstly, I would like to express my gratitude to Professor Hideaki Kasai for supervising my research. Indeed, I immensely indebted to all Kasai Laboratory members' support and encouragement that always helpful for reaching a sustainability of my research. Lastly, I would like to extend my appreciation to JASSO foundation under the Japan – East Asia Network of Exchange for Students &

Youths (JENESYS) Program for supporting my project.

REFERENCES

[1] Liu, H. J., Zhai J. P., Chan, C. T., Tang Z. K. (2007). *Adsorption of O_2 on a (4, 2) Carbon Nanotube*. Nanotechnology, vol. 18.

[2] Dresselhaus M S, Dressehaus G and Eklund P C. (1996). *Science of Fullenrenes and Carbon Nanotubes* (New York: Academic)

[3] Ebbesen T (ed) 1997 *Carbon Nanotube: Preparation and Properties* (Boca Raton, FL: CRC Press)

[4] Saito R, Dressehaus G and Dresselhaus M S. (1998). *Physics Properties of Carbon Nanotubes* (New York: World Scientific)

[5] Lu J P and Han J.(1998). *Int. J. High Electron. Syst. Vol.* 9, p. 101

[6] Kong J, Franklin N R, Zhou C, Chapline M G, Peng S, Cho K and Dai H. (2000). *Science vol.* 287, p. 622

[7] Collins P G, Bradley K, Ishigami M and Zettl A. (2000). *Extreme Oxygen Sensitivity of Electronic Properties of Carbon Nanotubes. Science vol.* 287, p. 1801-1804.

[8] Tang X P, Kleinhammes A, Shimoda H, Fleming L, Bennoune K Y, Sinha S, Bower C, Zhou O and Wu Y. (2000). *Science* **288** 492

[9] Sumanasekera G U, Adu C K W, Fang S and Eklund P C. (2000). *Phys. Rev. Lett.* **85** 1096

[10] Dean K A and Chalamala B R. (1999). *Appl. Phys. Lett.* **75** 3017

[11] Wadhawan A, Stallcup R E II and Perez J M.(2001). *Appl. Phys. Lett.* **78** 108

[12] Jhi S H, Louie S G and Cohen M L 2000 *Phys. Rev. Lett.* **85** 710

[13] Kong, Jing, Franklin, Nathan R., Zhou, Chongwu, Chapline, Michael G., Peng Shu. (2000). *Nanotube Molecular Wires as Chemical Sensors*. Science, vol. 28, p.622-625.

[14] Wang, Yun; T.W. Yeow, John. (2009). *A Review of Carbon Nanotubes- Based Gas Sensors*. Journal of Sensors, Hindawi Publishing Corporation.

[15] Charlier, Jean-Christophe; Blasé, Xavier; Roche, Stephan. (2007) *Electronic and Transport Properties of Nanotubes*. Reviews of Modern Physics, Vol. 79.

[16] Rafati, Amir Abbas; Hashemianzadeh, Seyed Majid; Nojini Zabiollah Bolboli. (2009) *Effect of the adsorption of oxygen on electronic structures and geometrical parameters of armchair single-wall carbon nanotubes: A density functional study*. Journal of Colloid and Interface Science, vol. 336, p.1-12.

MY LIFE EXPERIENCE IN JAPAN



Muhammad Aslam Bin Rosle

Kasai Laboratory, Department of Applied Physics, Graduate School of Engineering

Osaka University, 565-0871, JAPAN

There is no precious word other than gratefulness for being a part of the QEDC Short Term Program in Osaka University. Living as a research student within a year brought me thousands of memories in Japan. Since at the beginning, I would say that the great hospitality manifested by Japanese is really amazed me. Welcoming greetings with respectful words like *Yokoso*, *Konnichiwa* and extended with serving me 'ocha' or Japanese tea as well as friendly smiles make me feel honored. So, I believe such cordial reception and respecting guests are parts of Japanese culture's essence. These are why I did love Japan so much.



Candid moment at Ise-Ginja ***Snow memory at Nagano*** ***Gion Matsuri celebration***

In Japan, there are a lot of chances to learn, to work and to communicate with Japanese and other international students for being a professional researcher. The spirit of working collectively and supporting each other shown among Kasai Laboratory members really astonishingly motivated me to reach sustainable research. Although applied physics is not a part of my history study, but through earnest and continuous support from Professor Kasai truly ignite my enthusiast to keep moving forward involving this field of research in the future. Being as a research student, I experienced attending symposium, seminars, workshops,

classes, meeting as well as member discussions. So, I found these academic events are really beneficial as I learned sharing opinions, respecting other ideas, accepting critics and enhancing my research performance.

Memory with Japanese Lang. class members

One of Photo sessions after seminar

During my stay in Japan, many Japanese cultures and customs had been witnessed. From the daily life styles to special occasions, I found they are so amazing at their systematic systems, enlightened thoughts, and good ethics. In this thing, I am really happy that I could join some events such as Kobe Luminarie 2010, snowboards in Nagano Valley, Hanami Picnic, Fuji Mountain gazing, Gion Matsuri and Ise-Ginja with Japanese and other multi-national friends. Every event that we spent together brought me a full meaning about the everlasting friendship, self-development and also culture experience.

Hanami Party with Kasai Lab members

Finally, I am glad to have this golden opportunity to learn many things academically and socially. As life is going on, my life chapter in Japan may end here but the memories kept alive in my heart forever. Thank you to Prof. Kasai, Dino Sensei, my tutors, QEDC secretaries, and all Kasai Lab members for all your support.

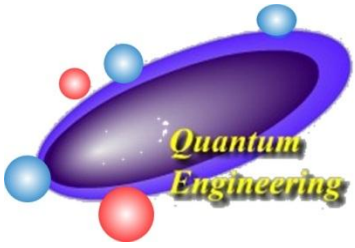

Quantum Engineering Design Research Initiative

Graduate School of Engineering, Osaka University

QEDRI office

Graduate school of Engineering, Osaka University
2-1 Yamadaoka, Suita, Osaka 565-0871, JAPAN
E-mail: qedc-staff@dyn.ap.eng.osaka-u.ac.jp

http://www.dyn.ap.eng.osaka-u.ac.jp/web/QED/index.html